

HIGH ENERGY SCATTERING AMPLITUDES
OF YANG-MILLS THEORY
IN THE EIGHTH ORDER.

by

C. Y. Lo

Submitted in Partial Fulfillment
of the Requirements for the
Degree of Doctor of
Science
at the

Massachusetts Institute of Technology

August 1976

lic. February 1977

Signature of Author

[Handwritten Signature]

Department of Physics, August 18, 1976

Certified by

[Handwritten Signature] Thesis Supervisor

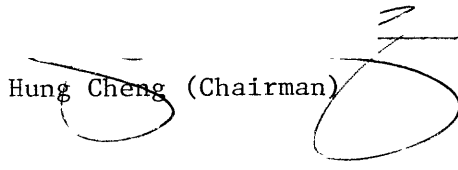
Accepted by

Chairman, Departmental Committee on
Graduate Students



This thesis has been examined by

✓
Hung Cheng (Chairman)



Felix M. H. Villars

Jeffrey E. Mandula

ABSTRACT

HIGH ENERGY SCATTERING AMPLITUDES

OF YANG - MILLS THEORY

BY

C. Y. LO

Submitted in Partial Fulfillment
of the Requirements for the
Degree of Doctor of
Science

We give the asymptotic forms of the amplitudes (up to the eighth order) for both fermion-fermion scattering and vector-meson-vector-meson scattering in the Yang-Mills theory with an iso-spin-1/2 Higgs boson in the limit $S \rightarrow \infty$ with t fixed.

We discuss the physical meaning of our results. We also suggest methods which will facilitate calculations in high-orders.

Thesis Supervisor: Hung Cheng



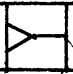





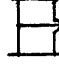





Title: Professor of Applied Mathematics

ACKNOWLEDGMENTS

I would like to express my sincere gratitude to Professor Hung Cheng, who suggested this problem and provided much unfailing guidance and understanding during the course of this work. Special acknowledgment is due to the National Science Foundation for financial support of this work. I also appreciate very much the encouragement, understanding and assistance from my teachers and friends during my stay at MIT.

Finally, I wish to thank Mrs. Natalie Alger, who did the typing, and Miss Inez Fung for her assistance in English.

TABLE OF CONTENTS

Chapter I	Introduction	7
Chapter II	Method of Calculation and notation	
§ 2.1	General Consideration	9
§ 2.2	Iso-Spin Factor of a Feynman diagram and a diagrammatic representation of an Iso-Spin factor	15
§ 2.3	Comparison of fermion-fermion scattering and vector-meson-vector-meson scattering	16
§ 2.4	Symmetry consideration	13
§ 2.5	Associate diagrams and iso-structure diagrams	19
§ 2.6	Two-dimensional transversal momentum diagrams.	20
§ 2.7	The magic of transforming a complicated integration into simple algebraic operations and illustrations of the sixth order calculations	21
Chapter III	Calculation of the eighth order diagrams	
§ 3.1	The ladder diagram 	30
§ 3.2	The diagram 	34
§ 3.3	The diagram 	36
§ 3.4	The diagram 	39
§ 3.5	The diagram 	40
§ 3.6	The diagram 	41
§ 3.7	The diagram  and the diagram 	41
§ 3.8	The diagram  and the diagram 	43
§ 3.9	Diagrams with only  contribution	44
§ 3.10	Diagrams with only  contribution	46
§ 3.11	The multi-vector meson exchange diagrams	47
§ 3.12	The cancellation of  terms	48
§ 3.13	The cancellation of  terms	49
§ 3.14	Terms of order greater than $S(\ln S)^3$	49
§ 3.15	Conclusion and discussion	49

Chapter IV	Higher order diagrams	
§4.1	The necessity of calculating higher order diagrams	53
§4.2	Convergent part of an integral and convergent diagrams	53
References		54
Appendix A	Feynman's rules	55
Appendix B	The Eighth order contributing diagrams	59

Chapter I Introduction

The study of various renormalizable field theories in the past few years has led to the abstraction of some general features applicable to high-energy hadron physics. Of particular interest in this area is the work of Cheng and Wu¹⁾ in quantum electro-dynamics (Q.E.D.). In their work, they predicted a rising total cross section, which was in turn supported by a recent Pisa-Stony experiment at CERN²⁾. Since Q.E.D. is a gauge theory, the question of whether the salient features of Q.E.D. are also possessed by non-abelian gauge theories, the Yang-Mills theories,³⁾ immediately comes to mind. Moreover, the possibility of constructing renormalizable Yang-Mills theories for weak and electro-magnetic interaction⁴⁾ and the discovery that non-abelian gauge theories are asymptotically free⁵⁾ make the study of the high-energy behaviors of Yang-Mills theories even more interesting.

In this thesis, we consider two-body elastic scatterings in terms of the usual Mandelstam invariant S (the square of the center of mass energy) and $t (= -\vec{\Delta}^2$ where $\vec{\Delta}$ is the momentum transfer). We study the high energy limits ($S \rightarrow \infty$ with $t \leq 0$ fixed) of non-abelian gauge fields.

Before we proceed, let us recall the work by Cheng and Wu¹⁾ in Q.E.D. They found the following: 1) In each perturbative order, all integrals over the transverse momenta converge. Therefore, all $\ln S$ factors arise from integrations over longitudinal momenta. 2) All the leading terms come from ladder-like diagrams and the sum of these leading terms violates the Froissart⁶⁾ bound. 3) To restore the Froissart bound, one needs to take into account of the exchange of two or more ladders.

The first published result of the high energy limit of non-abelian gauge field was given by Nieh and Yao⁷⁾. They stated that in the sixth

order perturbation theory the amplitude behaves as $S \ln^3 S$, whereas in the eighth order the amplitude behaves as $S \ln^5 S$. They also states that integrations in longitudinal and transverse phase space both contribute $\ln S$ factors.

They speculated that the amplitude is a power series in $\ln^2 S$ with alternating signs. They believed that the high energy behaviour of non-abelian theories can be drastically different from that of Q.E.D.

In this thesis, we use the approach of Cheng and Wu and go over the sixth order and eighth order calculations of Nieh and Yao. We find that our conclusions are totally in disagreement with those of Nieh and Yao. In particular, we find that high-energy scattering in Yang-Mills theory exhibits the same features as those found by Cheng and Wu in Q.E.D. Both the amplitude of fermion-fermion scattering and the amplitude of vector-meson-vector-meson scattering have been calculated. Our sixth order amplitude for fermion-fermion scattering agrees with that obtained by McCoy and Wu⁸⁾ somewhat earlier.

Finally, we discuss the physical meaning of our results. We also suggest methods which will facilitate calculations in high-orders.

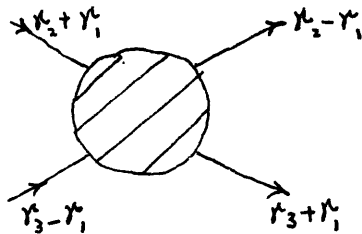
Chapter II Method of Calculation and Notation

§2.1 General Consideration

To be explicit, we shall restrict ourselves to the SU(2) Yang-Mills theory with an iso-spin-1/2 Higgs boson. Higgs mechanism is invoked so that there is no infrared divergence. The relevant Feynman rules for this theory have been given explicitly by t' Hooft and Veltman⁹⁾, using the procedure of Popov and Faddeev¹⁰⁾. We operate exclusively in the Feynman gauge where there are no $k_\mu k_\nu$ terms in the propagator for the Yang-Mills field. The Feynman rules are listed in Appendix A. We point out here that generalization to SU(N)¹¹⁾ is simple because the mechanism for the cancellation of many integrals is simply the Jacobi identity.

We will study the high energy scattering amplitude by means of the momentum space techniques, which were developed by Cheng and Wu¹²⁾, and which have been proven useful in studies of massive quantum electrodynamics. For detailed discussion of these methods, please refer to reference 12.

The essence of the momentum space method is that in the $S \rightarrow \infty$ limit a coordinate system is chosen such that large components of the momenta of the incoming and outgoing particles are along the z-axis. Let r_2+r_1 and r_3-r_1 be the momenta of the incoming particles, and r_2-r_1 and r_3+r_1 be those of the outgoing particles as shown below:



$$(2.1.1)$$

then we have approximately

$$r_2 \sim (w, w, 0) \text{ and } r_3 \sim (w, -w, 0) \quad (2.1.2)$$

where $w = 1/2 \sqrt{S}$. In such a coordinate system,

$$r_1 = (0, 0, \vec{r}_1) \quad (2.1.3)$$

We can take advantage (2.1.2) and (2.1.3) by introducing the variables¹²⁾

$$k^+ = k^0 + k^3 \text{ and } k^- = k^0 - k^3 \quad (2.1.4)$$

so that

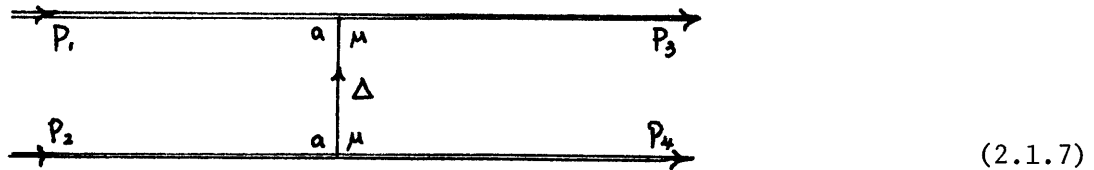
$$dk^0 dk^3 = (1/2) dk^+ dk^-, \quad (2.1.5)$$

Thus

$$\begin{aligned} r_2^+ &= 2w + 0(1/2w), \quad r_2^- = 0(1/2w), \\ r_3^+ &= 0(1/2w), \quad r_3^- = 2w + 0(1/2w), \\ r_1^\pm &= 0. \end{aligned} \quad (2.1.6)$$

and the basic approximation is to drop r_2^-, r_3^+, r_1^\pm and terms of $0(1/2w)$ whenever they occur in the Feynman integral.

As an example, we calculate the second and fourth order amplitudes of fermion-fermion scattering (the iso-spin of the fermion is 1/2). In the second order case there is only one dominant diagram



$$M_{ff}^{(2)} = (-i)(ig)^2(-i) \langle 3 | \frac{1}{2} \mathcal{C}_a \gamma^\mu | 1 \rangle \frac{-1}{\Delta^2 + \lambda^2} \langle 4 | \frac{1}{2} \mathcal{C}_a \gamma_\mu | 2 \rangle \quad (2.1.8)$$

Using the identity of the Gordon decomposition of current,

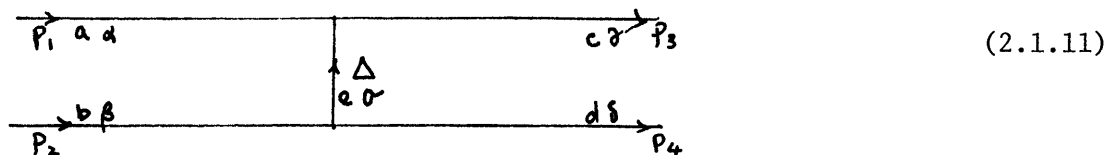
$$\bar{u}(p_3) \gamma^\mu u(p_1) = \bar{u}(p_3) \left[\frac{(p_1 + p_3)_\mu}{2M} + i \sigma^{\mu\nu} \frac{(p_3 - p_1)_\nu}{2M} \right] u(p_1) \quad (2.1.9)$$

and the equations in (3.1.6). We can approximate (2.1.8) such that

$$M_{ff}^{(2)} \cong g^2 \frac{1}{4} \langle 3 | \mathcal{C}_a | 1 \rangle \langle 4 | \mathcal{C}_a | 2 \rangle \frac{-1}{\Delta^2 + \lambda^2} \frac{S}{2M^2} \quad (2.1.10)$$

Notice that there is no spin flip in (2.1.10).

For the second order vector-meson-vector-meson scattering the dominant diagram is



$$(2.1.11)$$

with

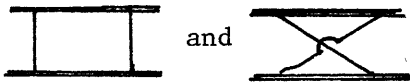
$$\begin{aligned} \mathcal{M}_{\nu\nu}^{(2)} = & (-i)(ig)^2(-i)\frac{-1}{\Delta^2+\lambda^2} E^*(3)_rc E(1)_{da} E^*(4)_{sd} E(2)_{\beta b} (i\epsilon_{aec})(i\epsilon_{bed}) \\ & \times \left\{ [g_{\alpha\sigma}(-P_1+\Delta)_\sigma + g_{\sigma\gamma}(-\Delta-P_3)_\alpha + g_{\gamma\alpha}(P_3+P_1)_\sigma] [g_{\beta\delta}(-P_2-P_4)_\sigma \right. \\ & \left. + g_{\delta\sigma}(P_4-\Delta)_\beta + g_{\sigma\beta}(\Delta+P_2)_\delta] + (\Delta^2+\lambda^2)(g_{\alpha\beta}g_{\gamma\delta} - g_{\alpha\delta}g_{\beta\gamma}) \right\} \quad (2.1.12) \end{aligned}$$

The high energy amplitude of vector-meson-vector-meson scattering is also non-spin-flip. It is easy to see that for non-zero helicity, the above expression can be simplified as the following:

$$\begin{aligned} \mathcal{M}_{\nu\nu}^{(2)} \sim & g^2 \frac{-1}{\Delta^2+\lambda^2} E^*(3)_c^r E(1)_a^d E^*(4)_d^s E(2)_b^\beta (\delta_{ab}\delta_{cd} - \delta_{ad}\delta_{bc}) \\ & (-1) g_{\sigma\alpha} g_{\beta\delta} (P_2+P_4) \cdot (P_3+P_1) \\ \sim & g^2 \frac{2s}{\Delta^2+\lambda^2} (\delta_{ab}\delta_{cd} - \delta_{ad}\delta_{bc}) E^*(4)_d^s g_{\alpha r} E(3)_c^r E^*(4)_d^s g_{\beta\delta} E(2)_b^\beta \quad (2.1.13) \end{aligned}$$

For each zero helicity incoming particle, an additional factor of $1/2$ ¹³ should be added to the scattering amplitude. We shall not show this case separately. From now on, we shall show the case of non-zero helicity only.

For fermion-fermion scattering the dominant fourth diagrams are



. Let us now calculate the first diagram

$$(2.1.14)$$

$$\begin{aligned} \mathcal{M}_{ff}^{(4)}(A) = & (-i)(ig)^4(-i)^4 \int \frac{d^4q}{(2\pi)^4} \langle s | \delta_{\nu\frac{1}{2}} \mathcal{O}_b(P_1+q_1+M) \delta^{\mu\frac{1}{2}} \mathcal{O}_a | 1 \rangle \frac{-1}{(P_1+q)^2-M^2+i\epsilon} \frac{1}{(P_2-q)^2-M^2+i\epsilon} \\ & \times \langle 4 | \delta_{\nu\frac{1}{2}} \mathcal{O}_b(P_2-q_1+M) \delta^{\mu\frac{1}{2}} \mathcal{O}_a | 2 \rangle \frac{1}{q^2-\lambda^2+i\epsilon} \frac{1}{(q-\Delta)^2-\lambda^2+i\epsilon} \quad (2.1.15) \end{aligned}$$

Now we integrate w.r.t. q^+ and denote q^- by Q . If $Q > P_2^- \sim 2w$, then the integration would be zero, since all the poles from the denominator lie in the lower half of the complex plane of q^+ . If $Q < -P_1^-$, then the integration would also be zero since all the poles from the denominator lie in the upper half of the complex plane of q^+ . Using the relation $P_1^\mu = 2P_1^- \delta^\mu_0$, (2.1.10) and (2.1.6), we have

$$\mathcal{M}_{ff}^{(A)} \sim (-i) g^4 2^{-2} \langle 3 | \mathcal{C}_b \mathcal{C}_a | 1 \rangle \langle 4 | \mathcal{C}_b \mathcal{C}_a | 2 \rangle \frac{S^2}{M^2} \\ \times \int \frac{d^4 q}{(2\pi)^4} \frac{1}{(P_1+q)^2 - M^2 + i\epsilon} \frac{1}{(P_2-q)^2 - M^2 + i\epsilon} \frac{1}{q^2 - \lambda^2 + i\epsilon} \frac{1}{(q-\Delta)^2 - \lambda^2 + i\epsilon} \quad (2.1.16)$$

If we close the integral in the upper (half) plane, then for the region $-P_1^+ < Q < 0$ there are three poles, $q^+ = \frac{q_1^2 + \lambda^2}{Q} + i\epsilon$, $q^+ = \frac{(q-\Delta)_1^2 + \lambda^2}{Q} + i\epsilon$ and $q^+ = P_2^+ - \frac{(\frac{1}{2}\Delta + q)_1^2 + M^2}{2W - Q} + i\epsilon$; and for the region $0 < Q < 2w$, there is only one pole $q^+ = P_2^+ - \frac{(\frac{1}{2}\Delta + q)_1^2 + M^2}{2W - Q} + i\epsilon$. For the region $-P_1^- < Q < 0$ the contribution from the first two poles are too small, so the net result will be that of the region $-P_1^- < Q < 2w$ with the pole $q^+ = P_2^+ - \frac{(\frac{1}{2}\Delta + q)_1^2}{2W - Q} + i\epsilon$

Now (2.1.16) becomes

$$\mathcal{M}_{ff}^{(A)} \sim 2^{-4} \langle 3 | \mathcal{C}_b \mathcal{C}_a | 1 \rangle \langle 4 | \mathcal{C}_b \mathcal{C}_a | 2 \rangle g^4 \frac{S^2}{M^2} (-i) (-2\pi i) \frac{1}{2} \int \frac{d^2 q_1}{(2\pi)^2} \int_{-P_1^-}^{P_2^-} dQ \frac{1}{2W} \\ \times \frac{1}{2W(Q+P_1^- - l + i\epsilon)} \frac{1}{-(q_1^2 + \lambda^2) + i\epsilon} \frac{1}{-(q-\Delta)_1^2 - \lambda^2 + i\epsilon} \\ \sim -2^{-5} \langle 3 | \mathcal{C}_b \mathcal{C}_a | 1 \rangle \langle 4 | \mathcal{C}_b \mathcal{C}_a | 2 \rangle g^4 \frac{S}{M^2} \int \frac{d^2 q_1}{(2\pi)^2} \frac{1}{q_1^2 + \lambda^2} \frac{1}{(q-\Delta)_1^2 + \lambda^2} \int_{-P_1^-}^{P_2^-} \frac{dQ}{Q + i\epsilon} \quad (2.1.17)$$

where $Q = [(q - \frac{1}{2}\Delta)_1^2 + M^2] / 2W$.

Now considering $P_1^- \sim 0(\frac{1}{2W})$, $P_2^- \sim 2w$, we have

$$\int_{-P_1^-}^{P_2^-} \frac{dQ}{Q + i\epsilon} = \int_{P_1^-}^{P_2^-} \frac{dQ}{Q} - i\pi \sim \int_{\frac{1}{2w}}^{2w} \frac{dQ}{Q} - i\pi = \ln 4 - i\pi \quad (2.1.18)$$

It thus follows that

$$\mathcal{M}_{ff}^{(A)} \sim -2^{-5} \langle 3 | \mathcal{C}_b \mathcal{C}_a | 1 \rangle \langle 4 | \mathcal{C}_b \mathcal{C}_a | 2 \rangle \frac{g^4}{M^2} \ln(4e^{-i\pi}) \\ \times \int \frac{d^2 q_1}{(2\pi)^2} \frac{1}{q_1^2 + \lambda^2} \frac{1}{(q-\Delta)_1^2 + \lambda^2} \quad (2.1.19)$$

The next diagram is

(2.1.20)

$$\mathcal{M}_{ff}^{(B)} = (-i) (ig)^4 (-i)^4 \int \frac{d^4 q}{(2\pi)^4} \langle 3 | \delta^{\mu\frac{1}{2}} \mathcal{C}_a(-P_3+q+M) \delta^{\nu\frac{1}{2}} \mathcal{C}_b | 1 \rangle \frac{1}{(P_3+q)^2 - M^2 + i\epsilon} \\ \times \langle 4 | \delta^{\mu\frac{1}{2}} \mathcal{C}_b(P_2-q+M) \delta^{\nu\frac{1}{2}} \mathcal{C}_a | 2 \rangle \frac{-1}{(P_2-q)^2 - M^2 + i\epsilon} \\ \times \frac{1}{q^2 - \lambda^2 + i\epsilon} \frac{1}{(q-\Delta)^2 - \lambda^2 + i\epsilon} \quad (2.1.21)$$

Calculations similar to those used in the previous case will reduce (2.1.21)

into

$$\begin{aligned}
 \mathcal{M}_{\mathcal{L}_{\mathcal{S}\mathcal{S}}}^{(4)}(B) &\sim -2^{-5} \langle 3 | \hat{c}_a \hat{c}_b | 1 \rangle \langle 4 | \hat{c}_b \hat{c}_a | 2 \rangle \frac{g^4}{M^2} (-s) \ln s \\
 &\times \int \frac{d^2 q_2}{(2\pi)^3} \frac{1}{q_2^2 + \lambda^2} \frac{1}{(q - \Delta)_2^2 + \lambda^2}
 \end{aligned}
 \tag{2.1.22}$$

For vector-meson-vector-meson scattering the dominant diagrams are

and . We calculate the first diagram

$$\begin{aligned}
 (A) \quad & \begin{array}{c} \xrightarrow{P_1 a \lambda} \quad \xrightarrow{P_1 + q} \textcircled{B} \quad \xrightarrow{P_3} \\ \xleftarrow{P_2 b \rho} \quad \xleftarrow{q} \textcircled{D} \quad \xleftarrow{q - \Delta} \textcircled{C} \quad \xleftarrow{q \delta P_4} \\ \xrightarrow{P_2 - q} \textcircled{A} \quad \xrightarrow{x} \end{array}
 \end{aligned}
 \tag{2.1.23}$$

Here we number each internal line and use the same number for time-spatial and iso-spin factor index since these indices will be summed up in different contexts. The amplitude is

$$\begin{aligned}
 \mathcal{M}_{VV}^{(4)}(A) &\sim (-i)(ig)^4 (-i)^4 \epsilon^{\alpha\beta\gamma\delta} \epsilon^{\alpha\beta\gamma\delta} \epsilon^{\alpha\beta\gamma\delta} \epsilon^{\alpha\beta\gamma\delta} \epsilon^{\alpha\beta\gamma\delta} \epsilon^{\alpha\beta\gamma\delta} \epsilon^{\alpha\beta\gamma\delta} \epsilon^{\alpha\beta\gamma\delta} \\
 &\int \frac{d^4 q}{(2\pi)^4} [g_{\alpha\lambda} (-P_1 + q)_3 + g_{13} (q - P_1 - q)_\alpha + g_{32} (P_1 + q + P_1)_1] \\
 & [g_{32} (-P_1 - q - q + \Delta)_8 + g_{27} (q - \Delta - P_3)_3 + g_{73} (P_3 - P_1 + q)_2] \\
 & [g_{\rho 4} (-P_2 - P_2 + q)_i + g_{4i} (P_2 - q - q)_\beta + g_{i\beta} (q + P_2)_4] \\
 & [g_{4\delta} (-P_2 + q - P_4)_2 + g_{\delta 2} (P_4 + q - \Delta)_4 + g_{24} (-q + \Delta + P_2 - q)_\delta] \\
 & \frac{1}{(P_1 + q)^2 - \lambda^2 + i\epsilon} \frac{1}{(P_2 - q)^2 + \lambda^2 + i\epsilon} \frac{1}{q^2 - \lambda^2 + i\epsilon} \frac{1}{(q - \Delta)^2 - \lambda^2 + i\epsilon}
 \end{aligned}
 \tag{2.1.24}$$

By (2.1.6) we have approximately

$$\begin{aligned}
 \mathcal{M}_{VV}^{(4)}(A) &\sim (-i) g^4 \epsilon^{\alpha\beta\gamma\delta} \epsilon^{\alpha\beta\gamma\delta} \epsilon^{\alpha\beta\gamma\delta} \epsilon^{\alpha\beta\gamma\delta} \epsilon^{\alpha\beta\gamma\delta} \epsilon^{\alpha\beta\gamma\delta} \epsilon^{\alpha\beta\gamma\delta} \epsilon^{\alpha\beta\gamma\delta} \\
 & g_{\alpha\lambda} (2P_1)_3 - 2P_2) g_{\rho\delta} (2P_1)_1 - 2P_2) \int \frac{d^4 q}{(2\pi)^4} \frac{1}{(P_1 + q)^2 - \lambda^2 + i\epsilon} \\
 & \frac{1}{(P_2 - q)^2 - \lambda^2 + i\epsilon} \frac{1}{q^2 - \lambda^2 + i\epsilon} \frac{1}{(q - \Delta)^2 - \lambda^2 + i\epsilon}
 \end{aligned}
 \tag{2.1.25}$$

We notice that (2.1.25) and (2.1.16) have almost the same integral except that all the particles have mass in (2.1.25). Simple substitution leads to

$$\begin{aligned}
 \mathcal{M}_{VV}^{(4)}(A) &\sim -\epsilon^{\alpha\beta\gamma\delta} g_{\rho\lambda} \epsilon^{\alpha\beta\gamma\delta} \epsilon^{\alpha\beta\gamma\delta} \epsilon^{\alpha\beta\gamma\delta} g_{\delta\rho} \epsilon^{\alpha\beta\gamma\delta} (i\epsilon_{\alpha 13} i\epsilon_{\beta 24} i\epsilon_{\gamma 41} i\epsilon_{\delta 24}) \\
 & g^4 2s \ln(s e^{-i\pi}) \int \frac{d^2 q_2}{(2\pi)^3} \frac{1}{q_2^2 + \lambda^2} \frac{1}{(q - \Delta)_2^2 + \lambda^2}
 \end{aligned}
 \tag{2.1.26}$$

Now we calculate the second diagram

$$(B) \quad \begin{array}{c} \xrightarrow{P_1 a \lambda} \quad \xrightarrow{-P_3 + q} \textcircled{B} \\ \xleftarrow{P_2 b \rho} \quad \xleftarrow{q} \textcircled{D} \quad \xleftarrow{q - \Delta} \textcircled{C} \\ \xrightarrow{P_2 - q} \textcircled{A} \quad \xrightarrow{x} \end{array}
 \tag{2.1.27}$$

Comparing (2.1.27) with (2.1.23), (2.1.20) and (2.1.14), we get

$$\begin{aligned}
M_{\nu\nu}^{(4)}(B) \sim & -\epsilon^{(3)c} g_{\nu\alpha} \epsilon^{(1)a} \epsilon^{(4)d} g_{\delta\beta} \epsilon^{(2)b} \epsilon^{(1)2} (i\epsilon_{c13} i\epsilon_{324} i\epsilon_{b41} i\epsilon_{a24}) \\
& \times g^4 2(-S) \ln S \int \frac{d^2 q_{\perp}}{(2\pi)^2} \frac{1}{q_{\perp}^2 + \lambda^2} \frac{1}{(q-\Delta)_{\perp}^2 + \lambda^2}
\end{aligned} \tag{2.1.28}$$

Up to the fourth order, the transverse momentum integrations converge. However, starting from the sixth order, the transverse momentum integrals contributed by some individual Feynman diagrams diverge. But we find that after all contributing diagrams of the same order are added together, the final integrals are convergent. This situation is entirely similar to the case of quantum electrodynamics. The mechanism for such drastic cancelations of divergent integrals is simply the Jacobi-identity. This point will be shown in Chapter III for the case of eighth order.

From the second to fourth order calculation the scattering amplitudes are non-spin-flip. This fact is also generally true for all orders (see §2.3) and is entirely similar to the case of Q.E.D.

For SU(2) we can express the non-spin-flip amplitude for fermion-fermion scattering as

$$M_{ff} = 2^{-5} M^{-2} (F_0 - \vec{\tau}^{(1)} \cdot \vec{\tau}^{(2)} F_1) \tag{2.1.29}$$

and the non-spin-flip amplitude for vector-meson-vector-meson scattering as

$$\begin{aligned}
M_{\nu\nu} = & \frac{1}{3} \delta_{ab} \delta_{cd} G_0 + \frac{1}{2} (\delta_{ac} \delta_{bd} - \delta_{ad} \delta_{bc}) G_1, \\
& + \frac{1}{2} (\delta_{ac} \delta_{bd} + \delta_{ad} \delta_{bc} - \frac{2}{3} \delta_{ab} \delta_{cd}) G_2
\end{aligned} \tag{2.1.30}$$

In the above, M is the mass of the fermion, S is the center-of-mass energy squared. $\vec{\tau}^{(i)}$, $i=1,2$ are the Pauli matrices for the isotopic spin of the fermion, and a and c (b and d) are the iso-spin indices of the incoming (outgoing) vector mesons. The invariant amplitudes F_n and G_n are so chosen that they are of I (iso-spin) = n in the t -channel, where $t = -\vec{\Delta}^2$, $\vec{\Delta}$ being the momentum transfer. It turns out that we have

$$F_1 = G_1$$

and

$$F_0 = (3/8) G_0 \tag{2.1.31}$$

§2.2 Iso-spin factor of a Feynman diagram and a diagrammatic representation of an iso-spin factor.

From the modified Feynman rules in Appendix A, we know that a Feynman diagram of $2n$ th order can be written in the following way.

$$M^{(2n)} = I \times g^{2n} (-i)(i)^{2n} (-i)^{3(n-1)+1} \int \prod_{j=1}^{n-1} \frac{d^4 q_j}{(2\pi)^4} \frac{N}{D} \tag{2.2.1}$$

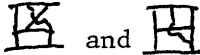
where I is the product of all the iso-spin factors of the vertices and the propagators and will be called the iso-spin factor of the diagram, and where $g^{2n} \frac{N}{D}$ is the product of the time-space parts and D is the product of the denominators from the propagators. Let us denote

$$\int \prod_{j=1}^{n-1} d^4 q_j \frac{N}{D} = (-2\pi i)^{n-1} \bar{N} / \bar{D} \tag{2.2.2}$$

Then we have

$$M^{(2n)} = I \times g^{2n} (-1/2)^{n-1} \int \prod_{j=1}^{n-1} \frac{d^2 q_{\perp j}}{(2\pi)^3} \int \prod_{i=1}^{n-1} dQ_i \bar{N} / \bar{D} \tag{2.2.3}$$

where Q_j denotes q_j^- to simplify notation and $q_{\perp j}$ is the transverse momentum of q_j .

We remark here that the sign of the iso-spin factor I depends not only on the diagram but also on the way it is drawn. For example, the iso-spin factors of  are different in sign. We use the Feynman diagram drawn to represent the iso-spin factor of the same Feynman diagram. Such representation enables us to do iso-spin calculation without referring to a particular group since the Jacobi-identity can be represented diagrammatically as follows:

$$\begin{array}{c} a \\ | \\ \text{---} \\ | \\ b \end{array}
 \begin{array}{c} c \\ | \\ \text{---} \\ | \\ d \end{array}
 =
 \begin{array}{c} a \\ \diagdown \\ \text{---} \\ \diagup \\ b \end{array}
 \begin{array}{c} c \\ \diagup \\ \text{---} \\ \diagdown \\ d \end{array}
 +
 \begin{array}{c} a \\ \text{---} \\ | \\ \text{---} \\ b \end{array}
 \begin{array}{c} c \\ \text{---} \\ | \\ \text{---} \\ d \end{array}
 \tag{2.2.4}$$

Also, the commutation relation can be represented by

$$\text{Diagram 1} = \text{Diagram 2} + \text{Diagram 3} \quad (2.2.5)$$

Obviously the assignment of iso-spin factor can be altered by a multiplicative constant. However, this is restricted by the following requirement that

$$\text{Diagram 1} = \text{Diagram 2} \quad (2.2.6)$$

The normalization requirement can be satisfied by changing the multiplicative constant such that we have

$$\text{Diagram 1} = 2 \delta_{ab} \quad (2.2.7)$$

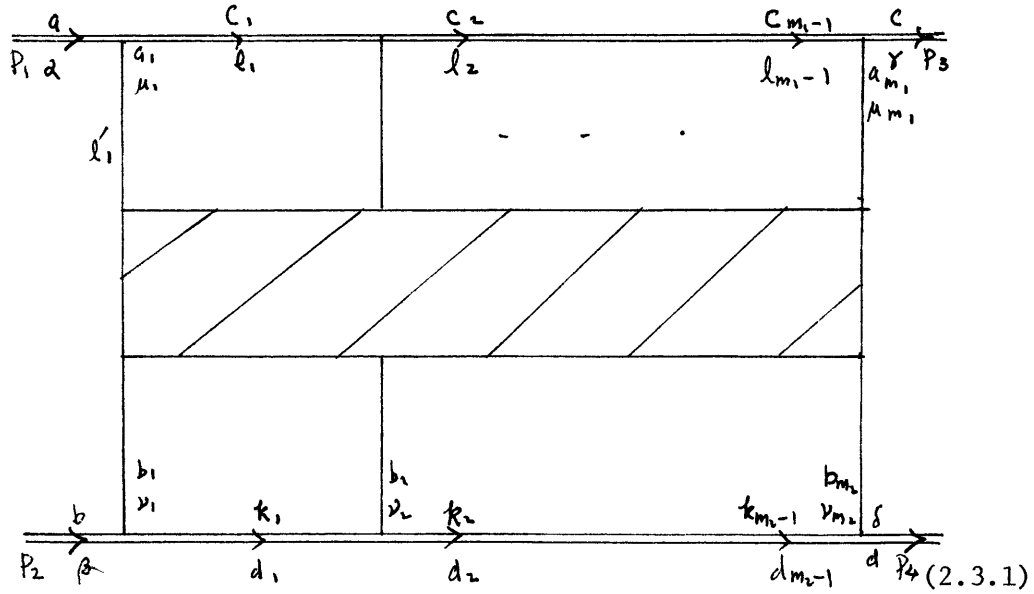
Relation (2.2.7) implies also

$$\text{Diagram 1} = \text{Diagram 2} \quad (2.2.8)$$

Of course, our iso-spin factors are normalized. We shall give a simple example of the power of Jacobi-identity in cancelling the divergent integrals in §2.7.

§2.3 Comparison of fermion-fermion scattering and vector-meson-vector-meson

scattering. We shall point out here that the calculations of the fermion-fermion scattering and the calculations of vector-meson-vector-meson scattering are essentially the same except for some difference in iso-spin factors. In section 2.1, we have given examples in the second and the fourth order. Let 1 and 2 be the incoming particles and 3 and 4 be the outgoing particles. Then a general $2n$ th order Feynman diagram can be represented in the following manner.



The corresponding amplitude is

$$\begin{aligned}
 \mathcal{M}_{ff}^{(2n)} &= (-i)(ig)^{m_1+m_2} (-i)^{m_1+m_2-2} \int \prod_{j=1}^{n-1} d^4q_j (2\pi)^{-4(n-1)} \\
 &\times \langle 3 | \delta^{\mu_{m_1} \frac{1}{2}} \mathcal{C}_{a_{m_1}}(k_{m_1}+M) \cdots \delta^{\mu_2 \frac{1}{2}} \mathcal{C}_{a_2}(k_1+M) \delta^{\mu_1 \frac{1}{2}} \mathcal{C}_{a_1} | 1 \rangle \\
 &\times \langle 4 | \delta^{\nu_{m_2} \frac{1}{2}} \mathcal{C}_{b_{m_2}}(k_{m_2}+M) \cdots \delta^{\nu_2 \frac{1}{2}} \mathcal{C}_{b_2}(k_1+M) \delta^{\nu_1 \frac{1}{2}} \mathcal{C}_{b_1} | 2 \rangle \\
 &\times \left(\prod_{i=1}^{m_1-1} \frac{-1}{l_i^2 - M^2 + i\epsilon} \right) \left(\prod_{i=1}^{m_2-1} \frac{1}{k_i^2 - M^2 + i\epsilon} \right) \times \text{[shaded box]} \quad (2.3.2)
 \end{aligned}$$

Relations (2.1.6), (2.1.9) and $P\delta^M = 2P^M - \delta^M P$ give the approximation,

$$\begin{aligned}
 \mathcal{M}_{ff}^{(2n)} &\sim ig^{m_1+m_2} \int \prod_{j=1}^{n-1} d^4q_j (2\pi)^{-4(n-1)} (-i)^{m_1+m_2-2} \frac{1}{2M^2} \left(\prod_{i=1}^{m_1-1} 2P_1^{\mu_i} \right) \left(\prod_{i=1}^{m_2-1} 2P_2^{\nu_i} \right) \\
 &\times \langle 3 | \frac{1}{2} \mathcal{C}_{a_{m_1}} \cdots \frac{1}{2} \mathcal{C}_{a_2} \frac{1}{2} \mathcal{C}_{a_1} | 1 \rangle \times \langle 4 | \frac{1}{2} \mathcal{C}_{b_{m_2}} \cdots \frac{1}{2} \mathcal{C}_{b_2} \frac{1}{2} \mathcal{C}_{b_1} | 2 \rangle \\
 &\times \left(\prod_{i=1}^{m_1-1} \frac{1}{l_i^2 - M^2 + i\epsilon} \right) \left(\prod_{i=1}^{m_2-1} \frac{1}{k_i^2 - M^2 + i\epsilon} \right) \times \text{[shaded box]} \quad (2.3.3)
 \end{aligned}$$

Now if we change all the fermion lines into vector meson lines, then the corresponding amplitude is approximately

$$\begin{aligned}
 \mathcal{M}_{vv}^{(2n)} &\sim ig^{m_1+m_2} \epsilon_{(3)c}^* g_{\delta\alpha} \epsilon_{(1)a}^d \epsilon_{(4)d}^e g_{\beta\gamma} \epsilon_{(2)b}^f \\
 &\times (i \epsilon_{a_1 c} i \epsilon_{c_1 a_1} \epsilon_2 \cdots i \epsilon_{c_{m_1-1} a_{m_1} c}) (i \epsilon_{\delta b_{m_2} d_{m_2-1}} \cdots i \epsilon_{d_2 b_2 d_1} i \epsilon_{d_1 b_1 b}) \\
 &\times \int \prod_{j=1}^{n-1} d^4q_j (2\pi)^{-4(n-1)} (-i)^{m_2} \left(\prod_{i=1}^{m_1-1} 2P_1^{\mu_i} \right) \left(\prod_{i=1}^{m_2-1} 2P_2^{\nu_i} \right) \\
 &\times \left(\prod_{i=1}^{m_1-1} \frac{1}{l_i^2 - \lambda^2 + i\epsilon} \right) \left(\prod_{i=1}^{m_2-1} \frac{1}{k_i^2 - \lambda^2 + i\epsilon} \right) \times \text{[shaded box]} \quad (2.3.4)
 \end{aligned}$$

We know that in the high energy approximation in the above integrals, the difference between masses λ and M is insignificant. It follows that the time-space parts of the two scattering are identical except for a constant factor. In order for a Feynman diagram to contribute to the leading $\ln S$ power, it is necessary that the lines attached to the top or the bottom line must be vector meson lines. It follows that there is a one-to-one correspondence between contributing diagram of fermion-fermion scattering and contributing diagram of vector-meson-vector-meson scattering. By comparing the identity (2.2.4), (2.2.5), (2.2.6) and (2.2.8) we conclude that it is sufficient to calculate one type of scattering and obtain the results for the other type by some simple iso-spin factor calculations. In this thesis we shall present the case of vector-meson-vector-meson scattering since this scattering has one more iso-spin channel.

§2.4 Symmetry consideration

The horizontal mirror image, or the vertical mirror image, of a diagram gives the same contribution as the original diagram. For the horizontal mirror image case, it is so simply because we get the same results when we integrate q^- first instead of q^+ . For the vertical mirror image case, it is so because if we change the direction of each momentum we get the same results.

Two diagrams are said to be mutually s-u symmetric if we obtain one of the diagrams when we rotate the top line of the other diagram w.r.t. a vertical axis, while keeping the rest of the vertices fixed. The amplitudes of two mutually s-u symmetric diagrams usually have very simple relations. This point can be seen very easily by comparing (2.1.19) and (2.1.26) with (2.1.22) and (2.1.28), respectively. Now let us define

$$(A, B) = (A (\ln s e^{-i\pi})^{n-1} + B (\ln s)^{n-1}) s / (n-1)! \quad (2.4.1)$$

and denote an iso-spin factor by $I(a, c; b, d)$. If the amplitude of a diagram is $I(a, c; b, d)(A, B)$, then the amplitude of its s-u symmetric diagram is usually $I(c, a; b, d)(-B, -A)$. However, there are exceptions to this rule. We shall explain this in §2.7. A set of diagrams is said to be independent if any two of them are not related by the above symmetric operations.

§ 2.5 Associate diagrams and iso-structure diagrams

According to the modified Feynman rules in Appendix A, any four-line vertex is denoted by two connecting three-line vertex with a bar on the connecting line. It follows that we can generate all the Feynman diagrams with four-line vertices by putting bars on Feynman diagrams with only three-line vertices in various fashions. However, this operation is subject to the following rules:

- 1) No two barred lines can join in a vertex.
- 2) No new vertex can be created other than those which appear in Appendix A.

Diagrams so generated are called associate diagrams of the original diagram. The advantage of such classification is that all associate diagrams have the same iso-spin factor as the original diagram. In the eighth order calculation, many diagrams contribute to terms higher than $s(\ln s)^3$, but these terms disappear if we add this diagram to its associate diagrams. This point will be explained in Chapter III.

Two diagrams are said to be iso-structure if they are identical when we change all lines into vector-meson lines. The advantage of such a classification is that the calculations of their time-space parts are very similar.

§ 2.6 Two-dimensional transverse momentum diagrams

It is convenient to represent multiple integrals over two-dimensional transverse momenta by diagrams which we shall call transverse momentum diagrams. These diagrams have vertices arranged in different vertical positions; they also have two outgoing lines (representing particles 1 and 3) on top and two incoming lines (representing particles 2 and 4) on the bottom, each pair carrying a transverse momentum Δ . An internal line of these diagrams represents a propagator $(\vec{q}_\perp^2 + \lambda^2)^{-1}$ where \vec{q}_\perp is the transverse momentum carried by the line. There is momentum conservation at each vertex, with the phase space factor $d^2q_\perp / (2\pi)^3$. The lines converging on a vertex from below (above) will be called incoming (outgoing) lines, and the sum of momentum directed toward a vertex carried by the incoming lines will be called the total momentum flow of the vertex. A horizontal bar on a vertex represents a factor $(\vec{q}_\perp^2 + \lambda^2)$ where \vec{q}_\perp is the total momentum flow of the point where the bar is located. Obviously, a bar on a line cancels the propagator. To clarify these points, we give the following examples:

$$\text{Diagram 1} = \int \frac{d^2q_\perp}{(2\pi)^3} \frac{1}{(\vec{q}_\perp^2 + \lambda^2)[(\vec{\Delta} - \vec{q}_\perp)^2 + \lambda^2]} \quad (2.6.1)$$

$$\text{Diagram 2} = \int \frac{d^2q_\perp}{(2\pi)^3} \frac{1}{(\vec{q}_\perp^2 + \lambda^2)} \quad (2.6.2)$$

$$\text{Diagram 3} = \int \frac{d^2q_\perp}{(2\pi)^3} \quad (2.6.3)$$

$$\text{Diagram 4} = \int \frac{d^2q_{1\perp} d^2q_{2\perp}}{(2\pi)^4} \frac{1}{(\vec{q}_{1\perp}^2 + \lambda^2)(\vec{q}_{2\perp}^2 + \lambda^2)[(\vec{\Delta} - \vec{q}_{1\perp} - \vec{q}_{2\perp})^2 + \lambda^2]} \quad (2.6.4)$$

$$\text{Diagram 5} = \left[\int \frac{d^2q_\perp}{(2\pi)^3} \frac{1}{(\vec{q}_\perp^2 + \lambda^2)[(\vec{\Delta} - \vec{q}_\perp)^2 + \lambda^2]} \right]^2 \quad (2.6.5)$$

$$\text{Figure 2.6.7} = \int \frac{d\vec{q}_{1L} d\vec{q}_{2L} d\vec{q}_{3L}}{(2\pi)^9} \frac{1}{(\vec{q}_{1L}^2 + \lambda^2)(\vec{q}_{2L}^2 + \lambda^2)(\vec{q}_{3L}^2 + \lambda^2)[(\vec{q}_{1L} + \vec{q}_{2L} - \vec{q}_{3L})^2 + \lambda^2]} \times \frac{(\vec{q}_{1L} + \vec{q}_{2L})^2 + \lambda^2}{(\Delta - \vec{q}_{1L} - \vec{q}_{2L})^2 + \lambda^2} \quad (2.6.7)$$

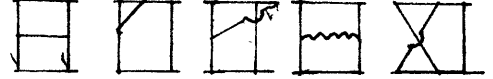
$$\text{Figure 2.6.8} = \int \frac{d\vec{q}_{1L} d\vec{q}_{2L} d\vec{q}_{3L}}{(2\pi)^9} \frac{1}{(\vec{q}_{1L}^2 + \lambda^2)(\vec{q}_{2L}^2 + \lambda^2)(\vec{q}_{3L}^2 + \lambda^2)[(\Delta - \vec{q}_{1L} - \vec{q}_{2L} - \vec{q}_{3L})^2 + \lambda^2]} \quad (2.6.8)$$

§2.7 The magic of transforming a complicated integration into simple

algebraic operations and illustrations of the sixth order calculations.

The Cheng-Wu method in calculating fourth order diagrams (see § 2.1) is essentially algebraic. We shall show here that the algebraic nature is also true for higher order calculations.

The dominant independent diagrams are



We shall calculate them one by one.

$$\text{Figure 2.7.1} \quad (2.7.1)$$

$$\mathcal{N}_1^{(6)} \sim \prod (-g)^6 \int \frac{d^4 q_1}{(2\pi)^4} \frac{d^4 q_2}{(2\pi)^4} \frac{N_1}{D_1}, \quad (2.7.2)$$

where

$$D_1 = [(P_1^+ + q_2^+) (P_1^- + q_2^-) - a_1 + i\epsilon] [(P_2^+ - q_1^+) (P_2^- - q_1^-) - a_2 + i\epsilon] \\ \times [a_3 q_2^+ - a_3 + i\epsilon] [a_4 q_2^+ - a_4 + i\epsilon] [a_5 q_1^+ - a_5 + i\epsilon] [a_6 q_1^+ - a_6 + i\epsilon] \\ \times [(a_1 - a_2)(q_1^+ - q_2^+) - a_7 + i\epsilon], \quad (2.7.3)$$

where $a_i = \vec{k}_{iL}^2 + \lambda^2$ and k_{iL} is the transverse momentum of the i th propagator,

and

$$N_1 = [g_{d3} (-P_1 + q_2)_1 + g_{31} (-2q_2 - P_1)_d + g_{1d} (2P_1 + q_2)_3] \\ \times [g_{14} (-P_1 - 2q_2 + \Delta)_8 + g_{48} (q_2 - \Delta - P_3)_1 + g_{r1} (P_3 + P_1 + q_2)_4] \\ \times [g_{35} (q_2 + q_1)_7 + g_{57} (-2q_1 + q_2)_3 + g_{73} (q_1 - 2q_2)_5] \\ \times [g_{76} (-2q_1 + q_2 + \Delta)_4 + g_{64} (q_1 + q_2 - 2\Delta)_7 + g_{47} (-2q_2 + \Delta + q_1)_6] \\ \times [g_{62} (-2q_2 + q_1)_5 + g_{25} (P_2 - 2q_1)_\beta + g_{5\beta} (q_1 + P_2)_2] \\ \times [g_{66} (P_4 + q_1 + \Delta)_2 + g_{62} (-2q_1 + \Delta + P_2)_8 + g_{25} (-2q_2 + q_1 - P_4)] \quad (2.7.4)$$

The integral over q_1^+, q_2^+ is zero unless

$$-\frac{1}{2w} \sim -P_1^- < Q_2 < Q_1 < P_2^- \sim 2w \quad (2.7.5)$$

We will then carry out the q_1^+ and q_2^+ integrals by closing on the poles.

$$q_1^+ = P_2^+ - \frac{a_2}{P_2^- - Q_1} + i\epsilon \quad \text{and} \quad q_2^+ = q_1^+ - \frac{a_7}{Q_1 - Q_2} + i\epsilon \quad (2.7.6)$$

It follows that

$$\begin{aligned} \bar{D}_1 \sim & [(P_1^+ + P_2^+ - \frac{a_2}{P_2^- - Q_1})(P_1^- + Q_2) - a_4 + i\epsilon] (P_2^- - Q_1) [\frac{a_2}{P_2^- - Q_1} - \frac{a_7}{Q_1 - Q_2} - a_3 + i\epsilon] \\ & [\frac{a_2}{P_2^- - Q_1} - \frac{a_7}{Q_1 - Q_2} - a_4 + i\epsilon] [\frac{a_1}{P_2^+ - Q_1} - a_5 + i\epsilon] \\ & [\frac{a_1}{P_2^+ - Q_1} - a_6 + i\epsilon] (Q_1 - Q_2) \end{aligned} \quad (2.7.7)$$

Before we go on, let us consider the following integrals

$$\int_{\frac{1}{2w}}^{2w} dx \int_{\frac{1}{2w}}^x dy \frac{1}{xy} = (\ln S)^2 / 2! \quad (2.7.8a)$$

$$\int_{\frac{1}{2w}}^{2w} dx \int_{\frac{1}{2w}}^x dy \frac{1}{y^2} \sim S \quad (2.7.8b)$$

$$\int_{\frac{1}{2w}}^{2w} dx \int_{\frac{1}{2w}}^x dy \frac{1}{x^2} \sim \ln S \quad (2.7.8c)$$

We note that for the above integral

$$\int_{\frac{1}{2w}}^{2w} dx \int_{\frac{1}{2w}}^x dy f(x, y) \sim \int_{\frac{1}{2w}}^{2w} dx \int_{\frac{1}{2w}}^x dy f(x, y) \quad (2.7.9c)$$

unless $a \ll 1$ or $b \ll 1$. It follows that the integration effective region is

just

$$\frac{1}{2w} < y \ll x \ll 2w \quad (2.7.10)$$

We know that

$$\frac{1}{x+i\epsilon} = \frac{1}{x} - i\pi \delta(x) \quad (2.7.11)$$

It follows that in our calculation we have

$$\int_{\frac{1}{2w}}^y \frac{dx}{x+i\epsilon} = \int_{\frac{1}{2w}}^y \frac{dx}{x} - i\pi \quad \int_{\frac{1}{2w}}^y \frac{dx}{x-i\epsilon} = \int_{\frac{1}{2w}}^y \frac{dx}{x} \quad (2.7.12)$$

Now we approximate (2.7.4) by dropping at the terms with coefficient

$O(1/2w)$, then we have

$$\begin{aligned} N_1 \sim & g_{\alpha\gamma} g_{\beta\delta} (-1)^{\frac{1}{2}} (4w)^{\frac{1}{2}} \left[-2a_7 - 2(g_1 + g_2 | g_1 + g_2 - 2\Delta)_{\perp} \right. \\ & \left. - 2q_1^+(Q_1 - 3Q_2) - 2q_2^+ Q_2 \right] \end{aligned} \quad (2.7.13)$$

We approximate \bar{N}_1 and \bar{D}_1 and get

$$\bar{N}_1 \sim -4S^2 [a_7 + (g_1 + g_2 | g_1 + g_2 - 2\Delta)_{\perp} + Q_2 a_7 / (Q_1 - Q_2)] \quad (2.7.14)$$

$$\bar{D}_1 \sim S(\alpha_2 + i\epsilon) \left[\alpha_2 \frac{a_7}{\alpha_1 - \alpha_2} + a_3 \right] \left[\alpha_2 \frac{a_7}{\alpha_1 - \alpha_2} + a_4 \right] a_5 a_6 (\alpha_1 - \alpha_2) \quad (2.7.15)$$

Now we separate the effective regions and consider them one by one.

There are only two regions:

$$\frac{1}{2}W < \alpha_2 \ll \alpha_1 \ll 2W \quad (2.7.16)$$

and

$$\frac{1}{2}W < \alpha_1 - \alpha_2 \ll \alpha_1 \ll 2W \quad (2.7.17)$$

In region (2.7.16) we have

$$\bar{N}_1 \sim -4S^2 \left[a_7 + (q_1 + q_2 / q_1 + q_2 - 2\Delta)_\perp \right]$$

$$\bar{D}_1 \sim S(\alpha_2 + i\epsilon) a_3 a_4 a_5 a_6 \alpha_1$$

It follows that in region (2.7.16)

$$\int d\alpha_1 d\alpha_2 \bar{N}_1 / \bar{D}_1 \sim \frac{-4S}{a_3 a_4 a_5 a_6} \frac{(\ln S - i\pi)^2}{2} \left[a_7 + (q_1 + q_2 / q_1 + q_2 - 2\Delta)_\perp \right] \quad (2.7.18)$$

In region (2.7.17) we have

$$\bar{N}_1 \sim -4S^2 \frac{\alpha_1}{\alpha_1 - \alpha_2} a_7$$

$$\bar{D}_1 \sim S(\alpha_1 + i\epsilon) \left(\frac{\alpha_1}{\alpha_1 - \alpha_2} a_7 \right)^2 a_5 a_6 (\alpha_1 - \alpha_2)$$

It follows that in region (2.7.17)

$$\int d\alpha_1 d\alpha_2 \bar{N}_1 / \bar{D}_1 \sim \frac{-4S}{a_5 a_6 a_7} \int d\alpha_1 d\alpha_2 \frac{1}{\alpha_1^2} \sim \frac{-4S}{a_5 a_6 a_7} \ln S$$

This contribution is very small compared with (2.7.18).

Therefore, the non-spin-flip amplitude for diagram (2.7.1) is

$$\mathcal{M}_1^{(6)} \sim \bar{H}^{(1)}(1, 0) \int \frac{d^2 q_{1,2}}{(2\pi)^3} \int \frac{d^2 q_{3,2}}{(2\pi)^3} \frac{[a_7 + (q_1 + q_2 / q_1 + q_2 - 2\Delta)_\perp]}{a_3 a_4 a_5 a_6} \quad (2.7.19)$$

After some simplification, we have



$$\mathcal{M}_1^{(6)} \sim \bar{H}^{(1)}(1, 0) \left[(3\lambda^2 + 2\bar{\Delta}^2) \mathcal{G} - 4\mathcal{G} \right] \quad (2.7.20)$$

The calculation of 2n order diagrams can be summarized as follows:


- 1) Draw the flow diagrams (as if $P_1^- = P_3^- = 0$) and pick up the poles.
- 2) Write down D and N by the Feynman rules, calculate \bar{D} and \bar{N} with the approximation $\alpha_i \ll 2W$ ($i = 1, \dots, n-1$).
- 3) List all the region of $0 < x_{n-1} \ll \dots \ll x_1 \ll 2W$, where x_i ($i = 1, \dots, n-1$)

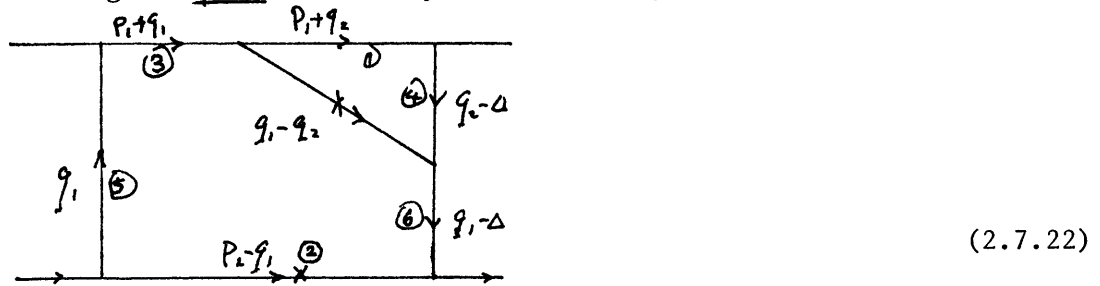
is a set of linearly independent linear combination of Q_i s. Then we calculate \bar{N}/\bar{D} in each region. Add all the contributions which are of order $(\ln S)^{n-1}$ or higher; simplify the integrals and represent them by two-dimensional transverse momentum diagrams.

Now we can see that all the calculations are algebraic. We shall illustrate these steps in the following calculations.

The diagram  and diagram  are iso-structure. Their denominators are almost the same (the mass λ and μ are different). They have the same flow diagram and the same set of poles but different numerator. Similar calculations show that the contribution is

$$\text{Diagram} (1, 0) (\lambda^2) \otimes \quad (2.7.21)$$

The next diagram  has only one flow diagram



Comparing with (2.7.1), the number 3 propagator is different

$$M_2^{(6)} \sim \text{Diagram} (-g^6) \int \frac{d^4 q_{12}}{(2\pi)^4} \int \frac{d^4 q_{21}}{(2\pi)^4} N_2/D_2 \quad (2.7.23)$$

We pick up the poles at line 2 and line 7.

$$q_1^+ = P_2^+ - \frac{a_2}{P_2 - a_1} + i\epsilon \sim \frac{\lambda^2 - 4t}{2W} - \frac{a_2}{2W - a_1} + i\epsilon \sim 0 + i\epsilon \quad (2.7.24)$$

$$q_2^+ = q_1^+ - \frac{a_7}{a_1 - a_2} + i\epsilon \sim -\frac{a_7}{a_1 - a_2} + i\epsilon \quad (2.7.25)$$

The denominator is

$$D_2 = [(P_1^+ + q_2^+)(P_1^- + a_2) - a_1 + i\epsilon] [(P_2^+ - q_1^+)(P_2^- - a_1) - a_2 + i\epsilon] \\ [(P_1^+ + q_1^+)(P_1^- + a_1) - a_3 + i\epsilon] [a_2 q_2^+ - a_4 + i\epsilon] [a_1 q_1^+ - a_5 + i\epsilon] \\ [a_1 q_1^+ - a_6 + i\epsilon] [(a_1 - a_2)(q_1^+ - q_2^+) - a_7 + i\epsilon] \quad (2.7.26)$$

$$N_2 \sim (4W)^5 (\frac{1}{2})^3 (2a_2 - a_1) = 8WS^2 (2a_2 - a_1) \quad (2.7.27)$$

Substituting $[(P_2^+ - q_1^+)(P_2^- - a_1) - a_2 + i\epsilon]$ and $[(a_1 - a_2)(q_1^+ - q_2^+) - a_7 + i\epsilon]$ by $(P_2^- - a_1)$ and $(a_1 - a_2)$ respectively and using relation (2.7.24)

(2.7.25), we transform D_2 into

$$\begin{aligned} \bar{D}_2 &\sim [2wQ_2 + i\epsilon][2w - Q_1][2wQ_1 + i\epsilon] \left[-Q_2 \frac{a_7}{Q_1 - Q_2} - a_4\right] [-a_5] [-a_6] (Q_1 - Q_2) \\ &\sim -2wS(Q_2 + i\epsilon)(Q_1 + i\epsilon) \left[Q_2 \frac{a_7}{Q_1 - Q_2} + a_4\right] a_5 a_6 (Q_1 - Q_2) \end{aligned} \quad (2.7.28)$$

For $Q_2 \ll Q_1$, we have

$$\begin{aligned} \bar{D}_2 &\sim -2wS a_4 a_5 a_6 Q_1^2 (Q_2 + i\epsilon) \\ \bar{N}_2 &\sim -8wS^2 Q_1 \end{aligned}$$

It follows that the integration of \bar{N}_2/\bar{D}_2 w.r.t. Q_1, Q_2 in this region is

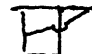
$$4S (\ln S e^{-i\pi}) / a_4 a_5 a_6 \quad (2.7.29)$$

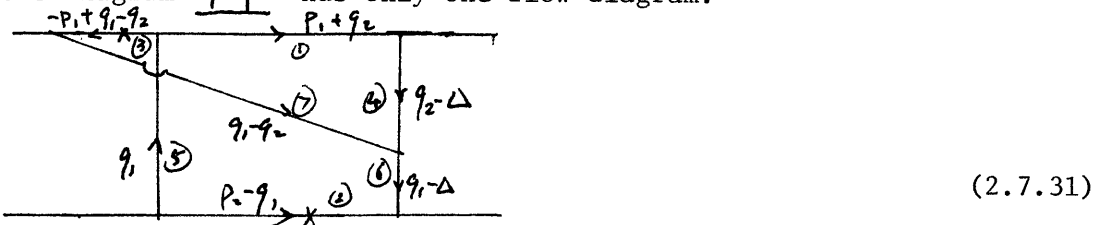
For $Q_2 \sim Q_1$ we have

$$\begin{aligned} \bar{D}_2 &\sim -2wS Q_1^2 (Q_1 - Q_2) Q_1 a_7 a_5 a_6 \\ \bar{N}_2 &\sim 8wS^2 Q_1 \end{aligned}$$

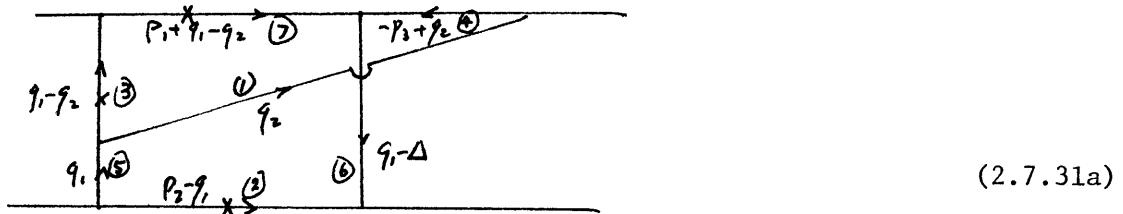
Now it is obvious that this region does not contribute. It follows that

$$M_2^{(6)} \sim \text{IV} (1, 0) \quad (2.7.30)$$

The next diagram  has only one flow diagram.



We either have the poles at line 2 and line 7 or the poles at line 2 and line 3. If we draw (2.7.31) differently by lifting lines 7 and 4 to the top, and lowering lines 3 and 1 we have



Mathematically (2.7.31) and (2.7.31a) are equal. But a pole at the top line of (2.7.31) shall make $q_2^+ \sim -2w$ and the standard approximation invalid.

If we wish to retain the standard approximation, we just switch to (2.7.31a) when we consider the poles at line 3 and line 2. In the case

fermion-fermion scattering the poles at the top (i.e. fermion line) are always suppressed, but then (2.7.31) and (2.7.31a) would be different Feynman diagrams, when we change the top and bottom lines into fermion lines. So there is still a one-to-one correspondence between diagrams of fermion-fermion scattering and vector-meson-vector meson scattering if we ignore the poles on the top line.

We pick the poles at line 2 and 7. Then we have

$$q_1^+ \sim 0, \quad \text{and} \quad q_2^+ \sim \frac{-q_7}{a_1 - a_2} \quad (2.7.32)$$

It follows that

$$\begin{aligned} \bar{D}_3 &\sim 2WS(a_1 - a_2)(a_2 + i\epsilon) a_5 a_6 \left[a_7 \frac{a_7}{a_1 - a_2} + a_4 \right] (a_1 - a_2) \\ \bar{N}_3 &\sim (4W)^5 \left(\frac{1}{2}\right)^3 (2a_2 - a_1) = 8WS^2 (2a_2 - a_1) \end{aligned} \quad (2.7.33)$$

For $Q_2 \ll Q_1$, we have

$$\begin{aligned} \bar{D}_3 &\sim 2WSQ_1^2 (a_2 + i\epsilon) a_5 a_6 a_4 \\ \bar{N}_3 &\sim -8WS^2 a_1 \\ \int \bar{N}_3 / \bar{D}_3 &\sim -4S \frac{(\ln S e^{i\pi})^2}{2!} \frac{1}{a_5 a_6 a_4} \end{aligned} \quad (2.7.34)$$

For $Q_1 - Q_2 \ll Q_1$, we have

$$\begin{aligned} \bar{D}_3 &\sim 2WS(a_1 - a_2) Q_1^2 a_5 a_6 a_7 \\ \bar{N}_3 &\sim 8WS^2 a_1 \\ \int \bar{N}_3 / \bar{D}_3 &\sim 4S \frac{(\ln S)^2}{2!} \frac{1}{a_5 a_6 a_7} \end{aligned} \quad (2.7.35)$$

The total contribution from the set of poles at lines 2 and 7 (by (2.23)), is

$$\int \bar{N}_3 / \bar{D}_3 (1, -1) (-1) \otimes \quad (2.7.36)$$

Now let us consider the poles at lines 2 and 3. We still have the same values,

$$q_1^+ \sim 0 \quad \text{and} \quad q_2^+ \sim \frac{-q_3}{a_1 - a_2}$$

since a_3 of (2.7.31a) is equal to a_7 of (2.7.31).


It is easy to see that

$$\bar{N}_{3a} = -\bar{N}_3 \quad (2.7.37)$$


The denominator is the same except $i\epsilon \leftrightarrow -i\epsilon$ for the propagator at the

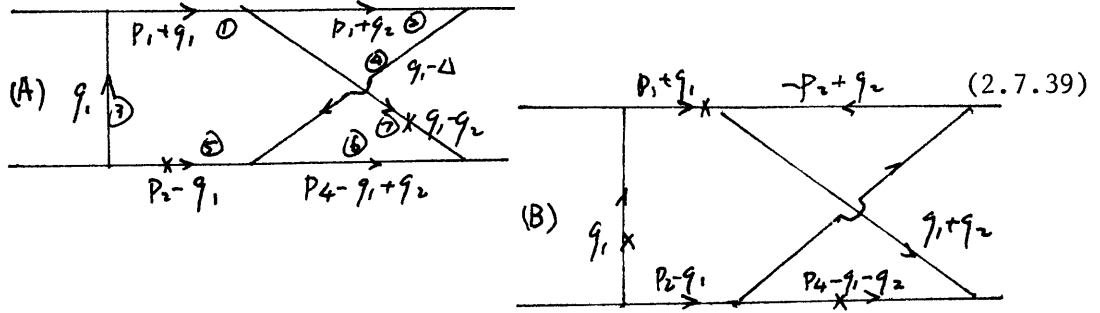
top. The contribution can be obtained from (2.7.36) by first exchanging the coefficients of $(\ln S)^2$ and $(\ln S e^{-i\pi})^2$ and then changing the sign.

The net result is that (2.7.36) remains the same and the total contribution

of Feynman diagram  is

$$N_3^{(6)} \sim \text{Diagram} (1, -1) (-2) \quad (2.7.38)$$

The multi-vector-meson exchange diagram  has two flow diagrams



From flow diagram (A) we have poles at line 5 and line 7,

$$\bar{N}_4 \sim (4w)^6 (-1)^3 \left(\frac{1}{2}\right)^3 = -8s^3$$

and

$$\bar{D}_4 \sim s^2 (Q_1 + i\epsilon) (Q_2 + i\epsilon) a_3 \left(a_2 \frac{-a_7}{a_1 a_2} - a_4 \right) (Q_1 - Q_2) \left(\frac{Q_7}{a_1 - a_2} \right)$$

The only contributing region is $Q_2 \ll Q_1$, then we have

$$\bar{D}_4 \sim -s^2 Q_1 (Q_2 + i\epsilon) a_3 a_4 a_7$$

It follows that

$$\int \bar{N}_4 / \bar{D}_4 \sim 8s \frac{(\ln S e^{-i\pi})^2}{2!} \frac{1}{a_3 a_4 a_7} \quad (2.7.40)$$

We have two sets of poles in flow diagram (B). However, the set with poles on lines 1 and 6 do not contribute, the remaining set is

$$q_1^+ = \frac{a_3}{Q_1} \quad \text{and} \quad q_2^+ \sim -q_1^+ = -\frac{a_3}{Q_1} \quad (2.7.41)$$

The numerator is also

$$\bar{N}_{4B} \sim -8s^3$$

and

$$\bar{D}_{4B} \sim s^2 (Q_1 + i\epsilon) Q_2 \frac{a_3}{Q_1} \left(a_2 \frac{a_3}{Q_1} + a_4 \right) a_7 Q_1$$

The only contributing region is $Q_2 \ll Q_1$, and we have

$$\overline{D}_{4B} \sim s^2 Q_1 Q_2 a_3 a_4 a_7$$

Hence,

$$\int \overline{N}_{4B} / \overline{D}_{4B} \sim -8s \frac{(\ln s)^2}{2!} \frac{1}{a_3 a_4 a_7} \quad (2.7.42)$$

Adding (2.7.40) and (2.7.41) we get the total contribution

$$M_4^{(6)} \sim \underline{IX} (1, -1) 2 \Phi \quad (2.7.43)$$

Since all the smallest Q_i are from a propagator on the top line s-u symmetry implies that the time-space part change from (A,B) to (B,A) $(-1)^{m-1}$ and iso-spin factor change from $I(a,c;b,d)$ to $I(c,a;b,d) (-1)^m$, when m is the number of vertices at the top line. The net result is

$$I(a,c;b,d)(A,B) \rightarrow -I(c,a;b,d)(B,A) \quad (2.7.44)$$

However, there are cases such that the contribution is not from a region where the smallest Q is not on the top line. Hence, (2.7.44) is not always true, although it is true for the sixth order diagrams. Counting all the symmetry, the total contribution from the sixth order diagrams

is

$$\begin{aligned} M_4^{(6)} \sim & \left[\left(\underline{H}(1,0) + \underline{K}(0,-1) \right) (3\lambda^2 + 2\bar{\Delta}^2) + \left(\underline{H}(1,0) + \underline{K}(0,-1) \right) (-\lambda^2) \right] \\ & \otimes + \left(\underline{IX} - \underline{JH} \right) (1,-1) 4 \Phi \\ & + 4 \left[(1,0) (-\underline{H} + \underline{IV} + \underline{VI}) + (0,-1) (-\underline{E} + \underline{V} - \underline{W}) \right] \otimes \quad (2.7.45) \end{aligned}$$

By Jacobi-identity (2.2.4), we can easily see that the iso-spin factor of the last term of (2.7.45) is zero.


Now we can see that in the sixth order the mechanism which keeps the transverse momentum integration convergent is the Jacobi-identity which is independent of the particular group used.

Chapter III Calculations of the eighth order diagrams

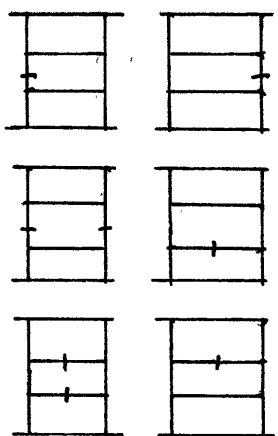
The calculations of the eighth order diagrams can easily exceed a thousand pages. It would be tedious to present to our readers the prohibitive wealth of details. We will, therefore, present here only those novel features of the calculations. Many straight forward simple calculations are omitted but the non-zero contribution of each diagram is listed. In order to explain that our result is not restricted to the particular group used, we use diagrams to represent iso-spin factors and show explicitly how the Jacobi-identity leads to cancellation of divergent transverse integrals. The eighth order amplitude is of order $S(\ln S)^3$, but for individual diagrams terms of order S^2 , $S^2 \ln S$ or S^3 do occur. By calculating a diagram and its associate diagrams together, such terms never appear in our calculation. But if we calculate these diagrams individually, errors are not easy to avoid since the highest order term is not $S(\ln S)^3$. Writing the contributions of each diagram into a sum of convergent integrals and divergent integrals where the numerator of the integrand is a constant, will help us to locate errors and thus eliminate them.

We shall see that in the eighth order, integration over the transverse momentum is also convergent although the cancellation of divergent integrals takes a much more complicated form. Let us define a diagram constructed by vector-meson lines with or without P-F ghost loops to be Yang-Mills diagram of first kind and the others to be Yang-Mills diagram of the second kind. In the eighth order, the total contribution from diagrams of the first kind, calculated with only the help of the Jacob-identity, is a sum of convergent integrals and a logarithmic divergent term with a coefficient proportional to λ^2 . The total

contribution from diagrams of the second kind is a sum of convergent integrals and a logarithmic divergent term with the coefficients of terms proportional to λ^2 . The logarithmic divergent λ^2 terms from diagrams of the first kind and diagrams of the second kind cancel each other.

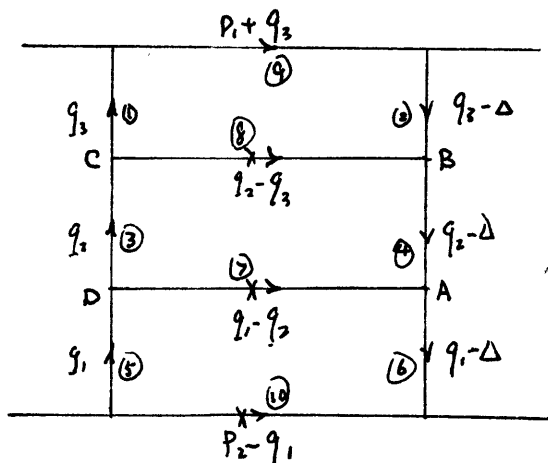
§3.1 The ladder diagram 

The following are its associate diagrams



Diagrams which have a bar in one of the lines associated with the top line or the bottom line are not presented here because such diagrams as a rule do not give contribution.

The ladder diagram has only one flow diagram as given below:



(3.1.1)

We label the vertices which are not on the top or bottom lines. We number the internal lines; and use a_i to denote $\vec{k}_i^2 + \lambda^2$ where \vec{k}_i is the transverse momentum of the i^{th} line and use a'_i to denote $(\vec{k}_i^2 + \mu^2)$. In this flow diagram we have a single pole (a pole is denoted by an x) at lines 7, 8 and 10. Diagrams with a bar on the line which has a pole will not contribute in our momenta space approximation technique. They actually give S^2 terms which are cancelled by the S^2 terms in the ladder diagram, which have been suppressed by momenta space approximation technique. In other words, we can ignore diagrams which have a bar on a pole. Hence, we have only three associate diagrams to consider.

Using (2.1.6) to approximate the denominator \bar{D} for the ladder diagrams, we have

$$\begin{aligned} \bar{D} \sim (2W)^2 (Q_3 + i\epsilon) & \left[Q_3 \left(\frac{a_7}{Q_1 - Q_2} + \frac{a_8}{Q_2 - Q_3} \right) + a_1 \right] \\ & \left[Q_3 \left(\frac{a_7}{Q_1 - Q_2} + \frac{a_8}{Q_2 - Q_3} \right) + a_2 \right] \left[Q_2 \frac{a_7}{Q_1 - Q_2} + a_3 \right] \left[Q_2 \frac{a_7}{Q_1 - Q_2} + a_4 \right] \\ & a_5 a_6 (Q_1 - Q_2)(Q_2 - Q_3) \end{aligned} \quad (3.1.2)$$

Using (2.1.6) to approximate the numerator N of the ladder diagram and its associate diagrams, we have

$$\begin{aligned} N \sim S^2 \{ & 2(-q_2^+) (-Q_2 + 2Q_3) [(-Q_1 + 2Q_2)(q_2^+ - q_3^+) + q_2^+ (-Q_1 + Q_2 + Q_3)] \\ & + (-q_2^+) (-Q_2 + 4Q_3) [2Q_3 + 2Q_4 + A(\beta)B(\beta)(-2) + C(\beta)D(\beta)(-2)] \\ & + 2(-Q_1 + 2Q_2) (-Q_2 + 2Q_3) (-q_2^+ \chi^2 q_2^+ - q_3^+) \\ & + 4(A(\alpha)D(\alpha))(B(\alpha)C(\alpha)) + 8(q_2^+)^2 (Q_2 - Q_3)^2 + 8a_3 a_4 \\ & + A(\alpha)B(\alpha)(-2) [2Q_3 + 2q_2^+ (Q_2 - Q_3)] + D(\alpha)C(\alpha)(-2) \\ & \times [2Q_4 + 2q_2^+ (Q_2 - Q_3)] + 2(-Q_2 + 2Q_3) (2q_2^+ - q_3^+) A(\alpha)D(\alpha)(-2) \\ & + 2(-Q_1 + 2Q_2) (-q_2^+) B(\alpha)C(\alpha)(-2) \\ & + (-Q_2 + 2Q_3) (-2q_2^+) [A(\alpha)C(\beta)(-2) + D(\alpha)B(\beta)(-2)] \\ & + (-q_2^+) (-2Q_2 + Q_3) [C(\alpha)A(\beta)(-2) + B(\alpha)D(\beta)(-2)] \}, \end{aligned}$$

$$\begin{aligned}
\text{where } A(\alpha) &= (q_1 + q_2 - 2\Delta)_\perp, & A(\beta) &= (-2q_1 + q_2 + \Delta)_\perp, \\
B(\alpha) &= (q_2 + q_3 - 2\Delta)_\perp, & B(\beta) &= (q_2 - 2q_3 + \Delta)_\perp, \\
C(\alpha) &= (q_2 + q_3)_\perp, & C(\beta) &= (q_2 - 2q_3)_\perp, \\
D(\alpha) &= (q_1 + q_2)_\perp, & D(\beta) &= (-2q_1 + q_2)_\perp.
\end{aligned} \tag{3.1.3}$$

The only regions of Q_1, Q_2, Q_3 space which can contribute to the maximum number of logarithms (i.e., $\ln^3 S$ and $i \ln^2 S$) are

$$2W \gg Q_1 \gg Q_2 \gg Q_3 > 0 \tag{3.1.4}$$

and

$$2W \gg Q_1 \sim Q_2, \quad \text{and} \quad Q_1 - Q_2 \gg Q_3 > 0 \tag{3.1.5}$$

In region (3.1.4) we have the approximation

$$\begin{aligned}
\bar{N} \sim S^{2,4} \{ & (a_7 + A(\alpha) D(\alpha)) (a_8 + B(\alpha) C(\alpha)) \\
& - (A(\alpha) B(\alpha) a_3 + D(\alpha) C(\alpha) a_4) + 2a_3 a_4 \}
\end{aligned} \tag{3.1.6}$$

In region (3.1.5) we have the approximation

$$\bar{N} \sim S^{2,4} \times 10 \left(Q_1 \frac{Q_2}{Q_1 - Q_2} \right)^2 \tag{3.1.7}$$

Integration with respect to Q_1, Q_2, Q_3 region (3.1.4) gives

$$\begin{aligned}
4(1,0) \{ & [a_7 + A(\alpha) D(\alpha)] [a_8 + B(\alpha) C(\alpha)] - [A(\alpha) B(\alpha) a_3 + C(\alpha) D(\alpha) a_4] \\
& + 2a_3 a_4 \} / a_1 a_2 a_3 a_4 a_5 a_6
\end{aligned} \tag{3.1.8}$$

and region (3.1.5) gives

$$10(1,0) / a_1 a_2 a_3 a_4 \tag{3.1.9}$$

After a lengthy calculation we find the total contribution of the ladder diagram and its associates are

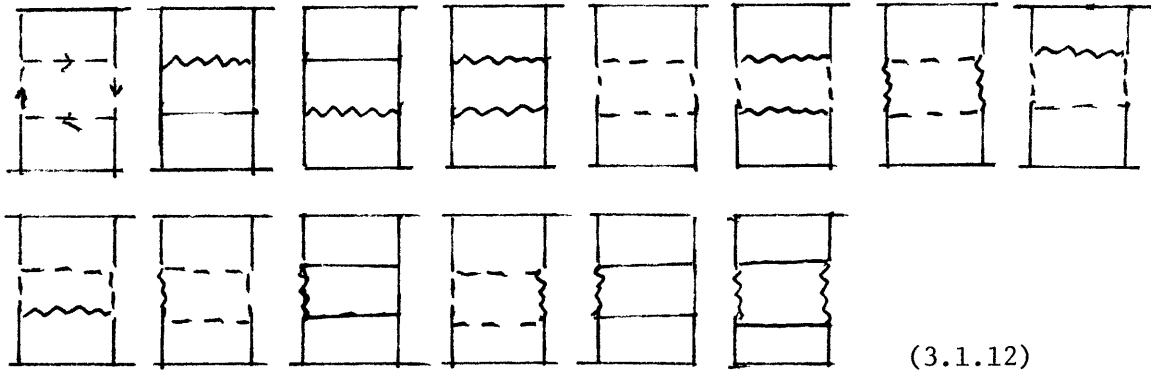
$$\begin{aligned}
& \left[\begin{array}{c} \text{---} \\ | \\ \text{---} \\ | \\ \text{---} \\ | \\ \text{---} \end{array} \right] (1,0) \left\{ \frac{1}{2} (2\Delta^2 + 3\lambda^2) \begin{array}{c} \text{---} \\ | \\ \text{---} \\ | \\ \text{---} \\ | \\ \text{---} \end{array} + (7\frac{1}{4} \Delta^2 + 11\lambda^2) \begin{array}{c} \text{---} \\ | \\ \text{---} \\ | \\ \text{---} \end{array} - 6 \begin{array}{c} \text{---} \\ | \\ \text{---} \\ | \\ \text{---} \end{array} \right. \\
& \left. - 3\frac{1}{4} \begin{array}{c} \text{---} \\ | \\ \text{---} \\ | \\ \text{---} \end{array} \right\}
\end{aligned} \tag{3.1.10}$$

Straight forward calculation shows that

$$\begin{array}{c} a \\ \text{---} \\ | \\ \text{---} \\ | \\ \text{---} \\ | \\ \text{---} \\ b \\ c \quad d \end{array} = (5\delta_{ab}\delta_{cd} + \delta_{ac}\delta_{bd} + 0\delta_{ad}\delta_{bc}) \tag{3.1.11}$$

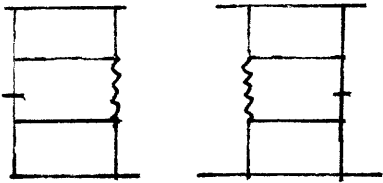
which we represent by the vector notation $(5,1,0)$.

The related diagrams of the ladder diagram are the following:



(3.1.12)

Their associate diagrams are:



(3.1.13)

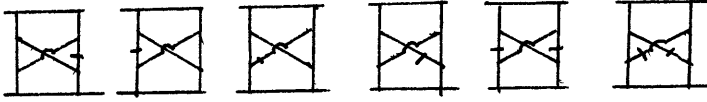
Simple calculations show that the contribution of the above diagrams are respectively

$$\begin{aligned}
 & \left[\text{Diagram 1} \right] (1, 0) \frac{1}{4} \text{Diagram 1}, \\
 & \left[\text{Diagram 2} \right] (1, 0) \lambda^2 \left[\frac{1}{2} (2\Delta^2 + 3\lambda^2) \text{Diagram 2} - 2 \text{Diagram 2} \right], \\
 & \left[\text{Diagram 3} \right] (1, 0) \frac{-\lambda^4}{2} \text{Diagram 3}, \\
 & \left[\text{Diagram 4} \right] (1, 0) \frac{1}{8} \text{Diagram 4}, \\
 & \left[\text{Diagram 5} \right] (1, 0) \frac{1}{8} \text{Diagram 5}, \\
 & \left[\text{Diagram 6} \right] (1, 0) \frac{1}{8} \text{Diagram 6}, \\
 & 2 \left[\text{Diagram 7} \right] (1, 0) \frac{1}{8} \text{Diagram 7}, \quad \text{and} \quad 2 \left[\text{Diagram 8} \right] (1, 0) \frac{1}{8} \text{Diagram 8}
 \end{aligned}$$

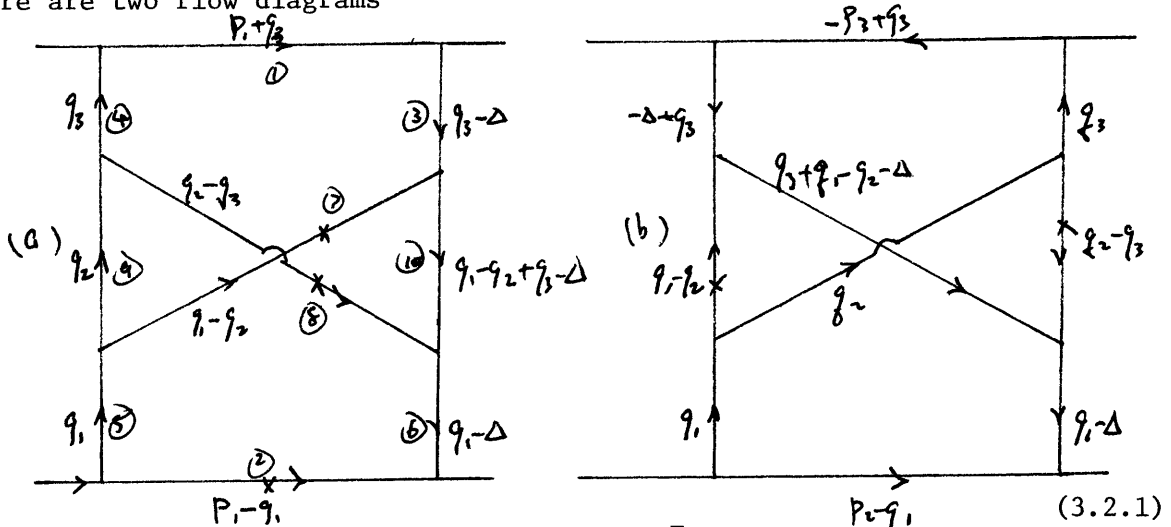
The last five diagrams do not contribute.

§ 3.2 The diagram

The associate diagrams are listed below:



There are two flow diagrams



Using (2.1.6) to approximate the denominator \bar{D} for flow diagram (a), we have

$$\begin{aligned} \bar{D} \sim s(\alpha_3 + i\epsilon) & \left[\alpha_3 \left(\frac{a_7}{\alpha_1 - \alpha_2} + \frac{a_8}{\alpha_2 - \alpha_3} \right) + a_3 \right] \left[\alpha_3 \left(\frac{a_7}{\alpha_1 - \alpha_2} + \frac{a_4}{\alpha_2 - \alpha_3} \right) + a_4 \right] \\ & a_5 a_6 (\alpha_1 - \alpha_2)(\alpha_2 - \alpha_3) \left[\alpha_2 \frac{a_7}{\alpha_1 - \alpha_2} + a_9 \right] \left[(\alpha_1 - \alpha_2 + \alpha_3) \frac{a_8}{\alpha_2 - \alpha_3} + a_{10} \right] \end{aligned} \quad (3.2.2)$$

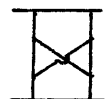
The important regions are

$$\alpha_1 \gg \alpha_2 \gg \alpha_3 \quad (3.2.3)$$

and

$$\alpha_1 \sim \alpha_2, \quad \alpha_1 - \alpha_2 \gg \alpha_3 \quad (3.2.4)$$


The contribution from region (3.2.3) is



$$\begin{aligned} & (1, 0) \frac{1}{4} \left\{ a_7 + a_8 + a_{10} - 4a_9 - \beta(A)\beta(B) - 2\alpha(C)\alpha(D) \right. \\ & \quad \left. + \alpha(C)(\alpha(B) - 2\beta(A)) + \alpha(D)(\alpha(A) - 2\beta(B)) \right\} \\ & \quad \times 1/a_3 a_4 a_5 a_6 a_9 \end{aligned} \quad (3.2.5)$$

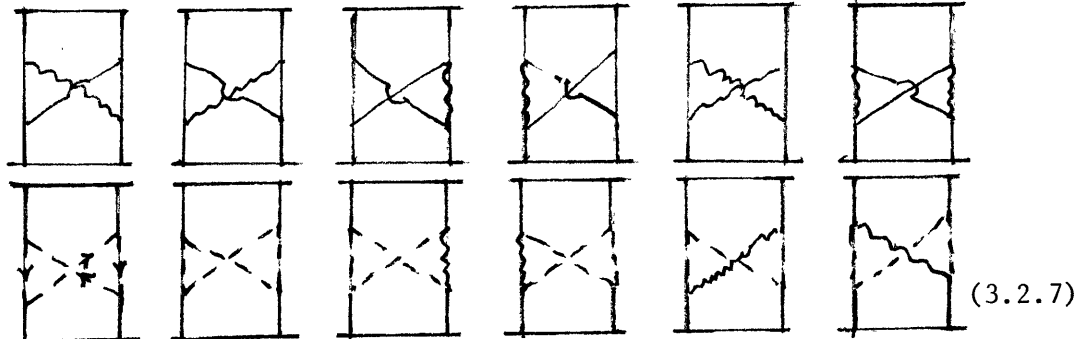
where $\alpha(D) = (q_2 + q_3)_\perp$, $\beta(D) = (q_2 - 2q_3)_\perp$,
 $\alpha(A) = (2q_1 - q_2 + q_3 - 2\Delta)_\perp$, $\beta(A) = (-q_1 - q_2 + q_3 + \Delta)_\perp$,
 $\alpha(B) = (q_1 - q_2 + 2q_3 - 2\Delta)_\perp$, $\beta(B) = (q_1 - q_2 - q_3 + \Delta)_\perp$,
 $\alpha(C) = (q_1 + q_2)_\perp$ and $\beta(C) = (q_2 - 2q_1)_\perp$.

The contribution from region (3.2.4) is the same as (3.2.5). Symmetry between flow diagrams (a) and (b) shows that the contribution from flow diagram (b) is equal to the contribution from flow diagram (a) after we make the substitution $S \rightarrow -S$.

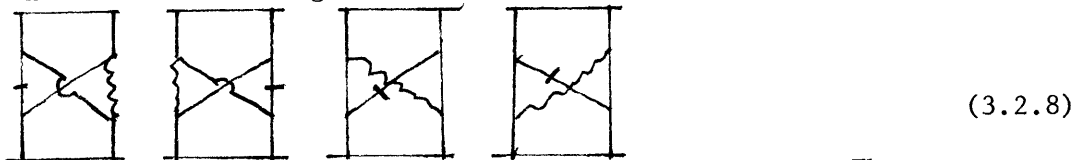
The total contribution from diagram  and its associates, after some simplification, is

$$\left[\text{Diagram} \right] (1, -1) \left[-\frac{1}{2} (6\frac{1}{2} \bar{\Delta}^2 + 11\lambda^2) \text{Diagram} + 6 \text{Diagram} + 3 \text{Diagram} \right] \quad (3.2.6)$$

The related diagrams are the following:



Their associate diagrams are:



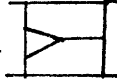
Only eight of the above diagrams give contributions. They are as

follows:

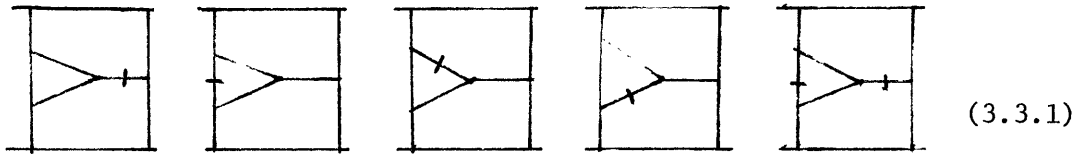
$$2 \left[\text{Diagram} \right] \left[(1, 0) \frac{\lambda^2}{2} + (0, -1) \frac{\lambda^2}{4} \right] \text{Diagram}$$

$$2 \left[\text{Diagram} \right] \left[(1, 0) \frac{-\lambda^2}{4} + (0, -1) \frac{-\lambda^2}{2} \right] \text{Diagram} \quad (3.2.9)$$

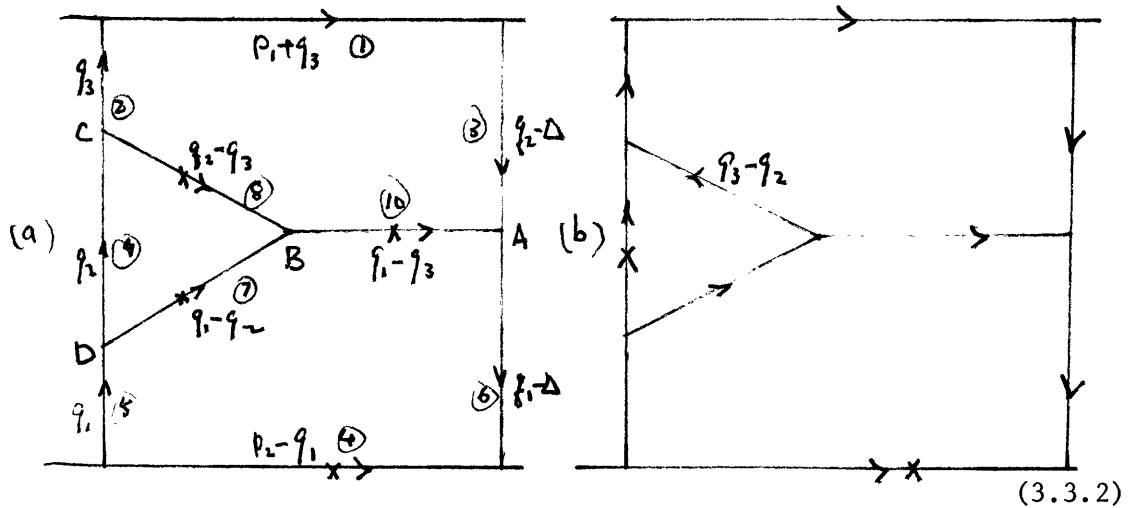
§ 3.3 The diagram



The associate diagrams are listed below:



There are two flow diagrams.



In flow diagram (a) we have two sets of poles to consider. For the set of poles at lines 4,7,8 our approximation gives

$$\begin{aligned} \bar{D} \sim & -(2W)^2 (a_3 + i\epsilon) \left[a_3 \left(\frac{a_7}{a_1 - a_2} + \frac{a_8}{a_2 - a_3} \right) + a_2 \right] \left[a_3 \left(\frac{a_7}{a_1 - a_2} + \frac{a_8}{a_2 - a_3} \right) + a_3 \right] \\ & a_5 a_6 (a_1 - a_2)(a_2 - a_3) \left[a_2 \left(\frac{a_7}{a_1 - a_2} \right) + a_9 \right] \\ & \left[(a_1 - a_3) \left(\frac{a_8}{a_2 - a_3} + \frac{a_7}{a_1 - a_2} \right) - a_{10} \right] \end{aligned} \quad (3.3.3)$$

The important regions are:

$$a_1 \gg a_2 \gg a_3 \quad (3.3.4)$$

and

$$a_1 \sim a_2, \quad a_1 - a_2 \gg a_3 \quad (3.3.5)$$

The contribution from region (3.3.4) is

$$\begin{aligned} (1, 0) \frac{1}{4} & \left[a_7 + a_8 + a_{10} + (q_1 + q_3 - 2\Delta | q_1 - 2q_2 + q_3)_{\perp} + (q_2 + q_3) q_2 + 3q_3 - 4\Delta \right]_{\perp} \\ & + (q_1 + q_2) 3q_1 - q_2 - 2q_3 - 4\Delta \right]_{\perp} + 7a_9 \Big/ a_2 a_3 a_5 a_6 a_9 \end{aligned} \quad (3.3.6)$$

The contribution from region (3.3.5) is

$$(1,0) \times 2 / a_2 a_3 a_5 a_6 \quad (3.3.7)$$

For the set of poles at lines 4,7,10 our approximation gives

$$\begin{aligned} \overline{D} \sim 3(a_3 + i\epsilon) \left[a_3 \frac{a_{10}}{a_1 - a_3} + a_2 \right] \left[a_3 \frac{a_{10}}{a_1 - a_3} + a_3 \right] a_5 a_6 (a_1 - a_2) \\ \left[(a_1 - a_2) \left(\frac{a_7}{a_1 - a_2} - \frac{a_{10}}{a_1 - a_3} \right) + a_9 \right] \left[a_2 \frac{a_7}{a_1 - a_2} + a_9 \right] (a_1 - a_3) \end{aligned} \quad (3.3.8)$$

The important region is

$$a_1 \sim a_2, \quad a_1 - a_2 \gg a_3 \quad (3.3.9)$$

and

$$a_1 \sim a_2, \quad a_3 \gg a_1 - a_2 \quad (3.3.10)$$

The contribution from region (3.3.9) is

$$(1,0) \left(\frac{1}{4} \right) / a_2 a_3 a_5 a_6 \quad (3.3.11)$$

The contribution from region (3.3.10) is

$$\overline{(0,-1)} \left(\frac{1}{4} \right) / a_2 a_3 a_5 a_6 \quad (3.3.12)$$

We would like to point out here that the contribution of this region is not subject to the s-u symmetry rule. The reason is that in region (3.3.10) the smallest variable $Q_1 - Q_2$ is not on the top line. The bar on top of the bracket is a notation to indicate such property.

In flow diagram (b) we have only one set of poles at lines 4,9,10.

Our approximation gives

$$\begin{aligned} \overline{D} \sim 5(a_3 + i\epsilon) \left[a_3 \frac{a_{10}}{a_1 - a_3} + a_2 \right] \left[a_3 \frac{a_{10}}{a_1 - a_3} + a_3 \right] a_5 a_6 a_2 (a_1 - a_2) \\ \left[(a_1 - a_2) \frac{a_9}{a_2} + a_7 \right] \left[(a_3 - a_2) \left(\frac{a_{10}}{a_1 - a_3} + \frac{a_9}{a_2} \right) + a_5 \right] \end{aligned} \quad (3.3.13)$$

The important region is

$$a_1 \gg a_3 \gg a_2 \quad (3.3.14)$$

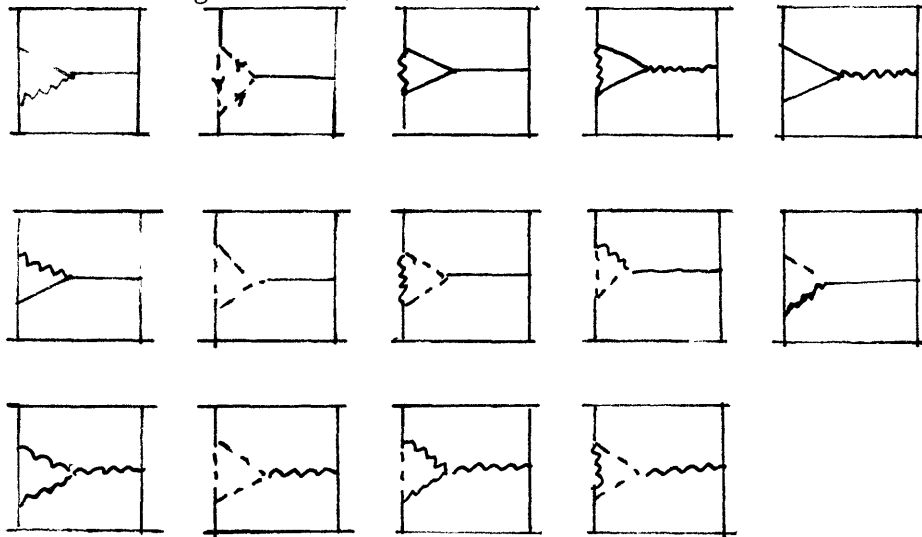
It gives a contribution

$$(1,-1) \frac{1}{8} / a_2 a_3 a_5 a_6 \quad (3.3.15)$$

After simplification the total contribution from the above diagrams is

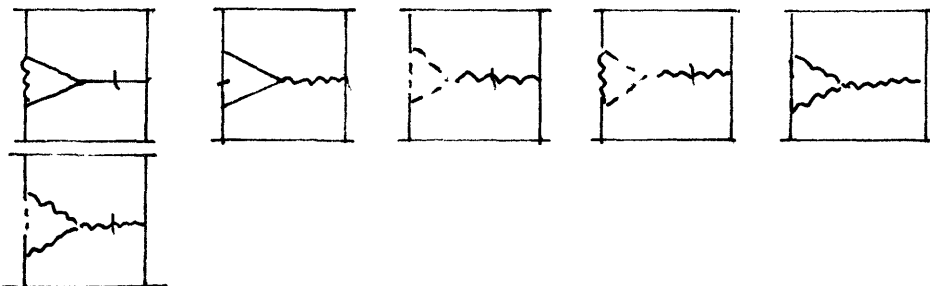
$$\left[\text{Diagram} \right] \left\{ (1, 0) \left[-\frac{1}{4} (6\frac{1}{2} \Delta^2 + 11 \lambda^2) \right] + 3 \left[\text{Diagram} \right] + 4 \left[\text{Diagram} \right] + \overline{(0, -1)} \frac{1}{8} \left[\text{Diagram} \right] \right\} \quad (3.3.16)$$

The related diagrams are:



(3.3.17)

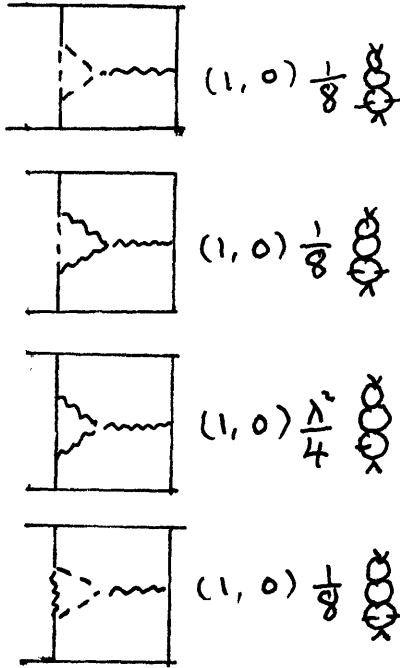
Their associate diagrams are:





(3.3.18)

Similar calculations show that they give the following contributions.

$$\begin{aligned}
 & \left[\text{Diagram} \right] (0, -1) \frac{1}{8} \left[\text{Diagram} \right] \\
 & 2 \left[\text{Diagram} \right] (1, 0) \frac{\lambda^2}{4} \left[\text{Diagram} \right] \\
 & \left[\text{Diagram} \right] (1, 0) \frac{\lambda^2}{8} \left[\text{Diagram} \right]
 \end{aligned}$$



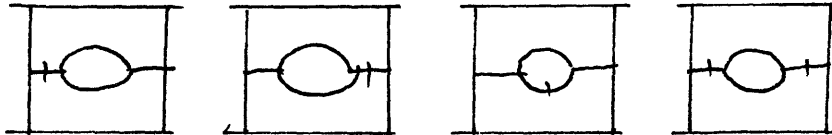
(3.3.19)

Now we can see that the contribution of diagram  cancels the bar term in the contribution of diagram . If we have considered these two diagrams together at the beginning, there would not be bar term contribution. In other words when considering a diagram, we always, at the same time, consider related diagrams with all the possible F-P ghost loops.

§3.4 The diagram

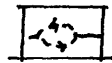


The associate diagrams are listed below:



(3.4.1)

There is one F-p ghost loop diagram

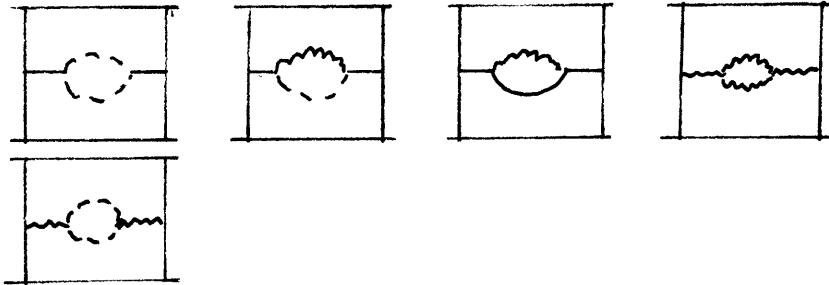


The above diagram gives the following contribution

$$\frac{1}{2} \times (1, 0) (-5) \times$$

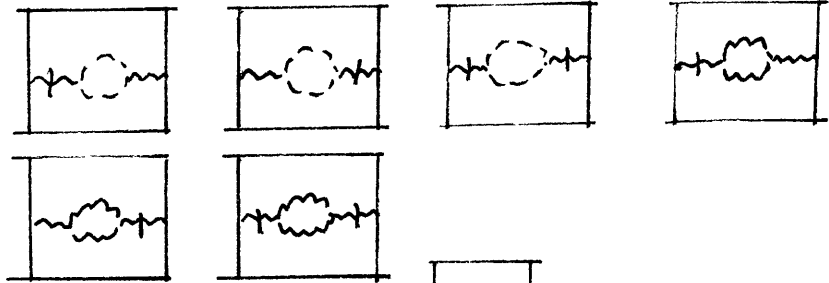
(3.4.2)

The related diagrams are:



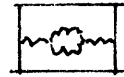
(3.4.3)

Their associate diagrams are



(3.4.4)

The contribution from diagram

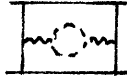


is

$$\frac{1}{2} \left[\text{diagram} \right] (1,0) = \frac{1}{4} \left[\text{diagram} \right]$$

(3.4.5)

The contribution from diagram



is

$$\frac{1}{2} \left[\text{diagram} \right] (1,0) = \frac{1}{4} \left[\text{diagram} \right]$$

(3.4.6)

The first three related diagrams and their associates together with diagram



and diagram



give the following contribution

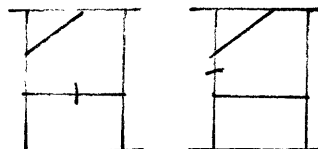
$$\left[\text{diagram} \right] (1,0) = \frac{1}{2} \left[\text{diagram} \right]$$

(3.4.7)

§3.5 The diagram



The associate diagrams are listed below:




(3.5.1)

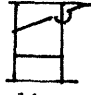
They give the following contribution

$$\left[\text{diagram} \right] (1,0) \left\{ -\frac{1}{2} (2\bar{\Delta}^2 + 3\lambda^2) \left[\text{diagram} \right] + 2 \left[\text{diagram} \right] \right\}$$

(3.5.2)

The related diagram  gives the following contribution

$$(1, 0) \frac{\lambda'}{2} \text{diagram} \quad (3.5.3)$$

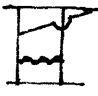
§3.6 The diagram 

The associate diagrams are



$$\text{diagram} \quad \text{diagram} \quad (3.6.1)$$

They give a contribution

$$(1, -1) \left[\frac{1}{2} (2\Delta^2 + 3\lambda') \text{diagram} - 2 \text{diagram} \right] \quad (3.6.2)$$

The related diagram  gives the following contribution

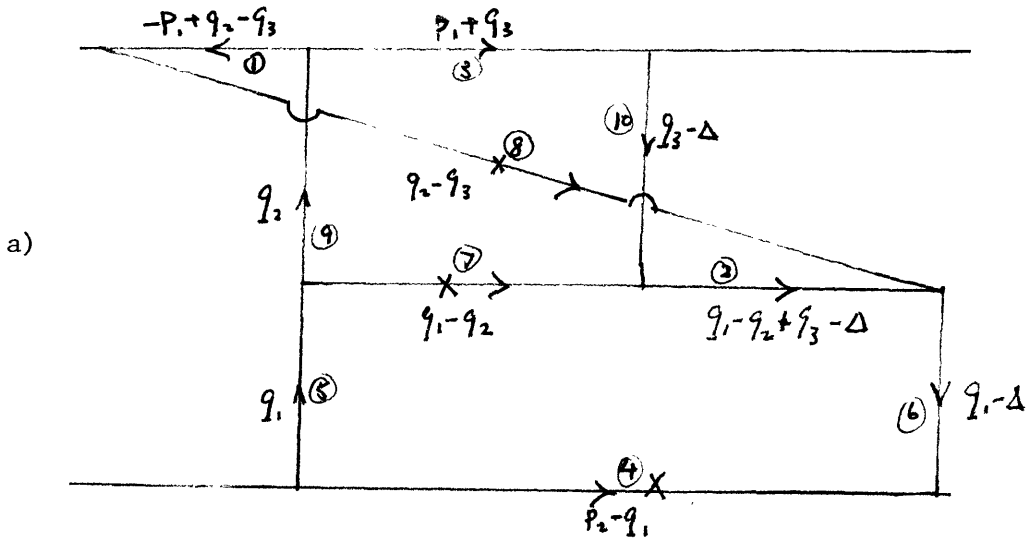
$$(1, -1) \frac{-\lambda'^2}{2} \text{diagram} \quad (3.6.3)$$

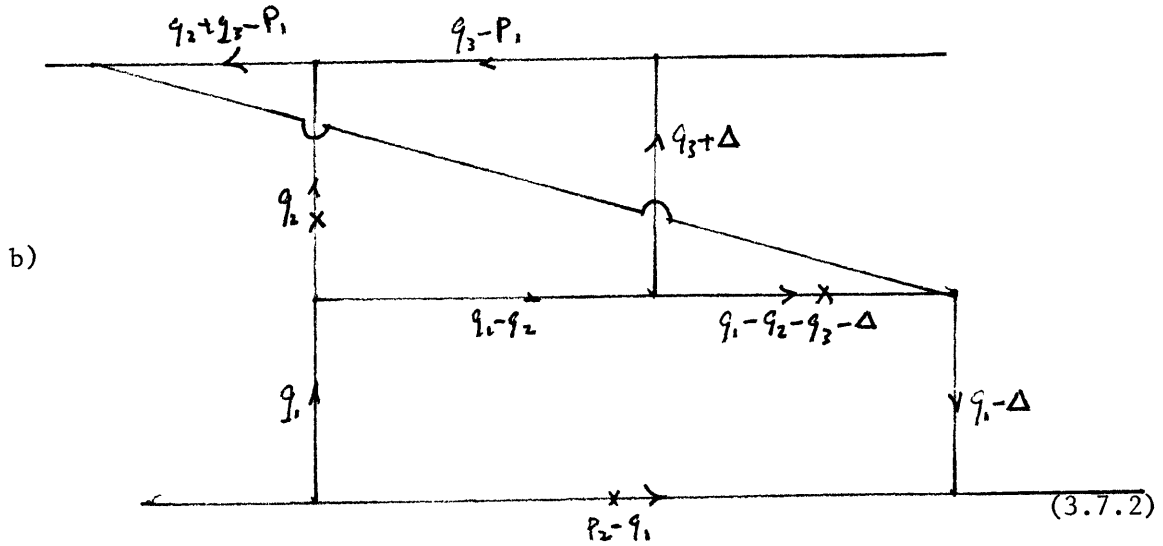
§3.7 The diagram  and the diagram 

The associate diagrams are

$$\text{diagram} \quad \text{diagram} \quad (3.7.1)$$

It has two flow diagrams





In flow diagram (a) we have poles at lines 4,7 and 8. Our approximation gives

$$\begin{aligned} \bar{D} &\sim (2W)^2 (\alpha_2 - \alpha_3) (\alpha_3 + i\epsilon) \left[(\alpha_1 - \alpha_2 + \alpha_3) \frac{a_8}{\alpha_2 - \alpha_3} + a_2 \right] \\ &\quad a_5 a_6 (\alpha_1 - \alpha_2) (\alpha_2 - \alpha_3) \left[\alpha_2 \frac{a_7}{\alpha_1 - \alpha_2} + a_9 \right] \\ &\quad \left[\alpha_3 \left(\frac{a_7}{\alpha_1 - \alpha_2} + \frac{a_8}{\alpha_2 - \alpha_3} \right) + a_{10} \right] \end{aligned} \quad (3.7.3)$$

The important regions are

$$\alpha_1 \gg \alpha_2 \gg \alpha_3 \quad (3.7.4)$$

$$\alpha_1 \gg \alpha_2 \sim \alpha_3 \quad (3.7.5)$$

and

$$\alpha_1 \sim \alpha_2, \quad \alpha_1 - \alpha_2 \gg \alpha_3 \quad (3.7.6)$$

When integrating \bar{N}/\bar{D} w.r.t. $\alpha_1, \alpha_2, \alpha_3$ these regions give respectively the following contributions:

$$2(1,0) \left\{ a_8 + 2 \left[a_7 + a_2 - \alpha(A) \beta(B) + \alpha(C) (\beta(B) - 2\alpha(A)) \right] \right\} \times 1 / a_5 a_6 a_8 a_9 a_{10} \quad (3.7.7)$$

$$2(0,-1) / a_5 a_6 a_8 a_9 \quad (3.7.8)$$

$$2(1,0) / a_2 a_5 a_6 a_{10} \quad (3.7.9)$$

where

$$\begin{aligned} \alpha(A) &= (-q_1 - q_2 + q_3 + \Delta)_{\perp}, & \alpha(B) &= (q_1 - q_2 + 2q_3 - 2\Delta)_{\perp}, \\ \beta(B) &= (q_1 - q_2 - q_3 + \Delta)_{\perp}, & \text{and } \alpha(C) &= (q_1 + q_2)_{\perp}. \end{aligned}$$

In flow diagram (b) we have poles at lines 4,9,2. The important regions are

$$Q_1 \gg Q_2 \gg Q_3 \tag{3.7.10}$$

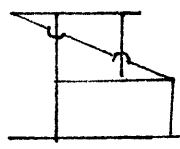
and

$$Q_1 \sim Q_2 \gg Q_3 \tag{3.7.11}$$

These two regions give the same contribution as region (3.7.4) and (3.7.6)

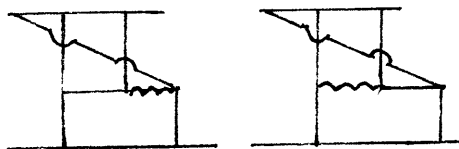
if we make a $S \rightarrow -S$ substitution

Total contribution after some simplification is



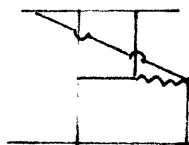
$$\left\{ (1, -1) \left[\frac{1}{2} (4\bar{\Delta}^2 + 7\lambda^2) \text{diagram} - 3 \text{diagram} - 2 \text{diagram} \right] + (0, -1) \frac{1}{4} \text{diagram} \right\} \tag{3.7.12}$$

The related diagrams are:



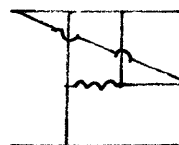
$$\tag{3.7.13}$$

They give the following contributions


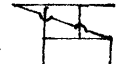


$$(1, -1) \frac{-\lambda^2}{2} \text{diagram} \tag{3.7.14}$$


and



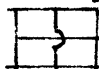

$$(1, -1) \frac{-\lambda^2}{2} \text{diagram} \tag{3.7.15}$$

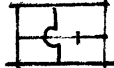
Diagram  has the topological structure as diagram 

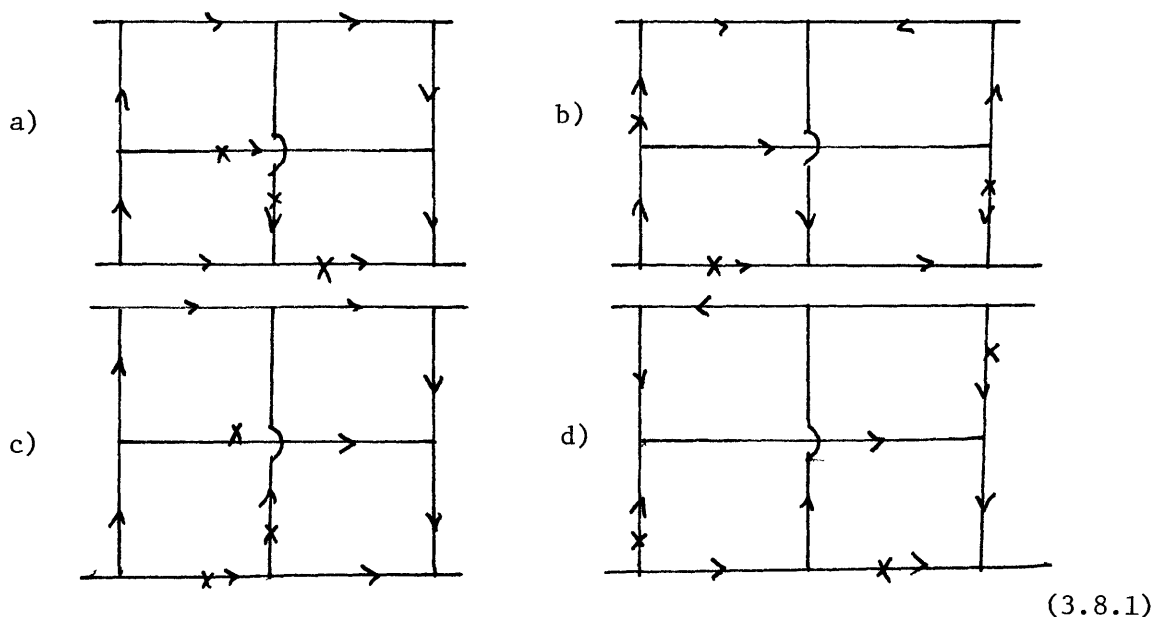
and give the following contribution



$$(1, 0) \frac{1}{2} \text{diagram}$$

§ 3.8 The diagram  and the diagram 

It has one associate diagram  but four flow diagrams.



It can be shown that flow diagrams (a) and (b) give the same contribution as (c) and (d).

and its associate give the following contribution

$$(1, -1) \left[-4 \text{ (bubble)} - 2\lambda^2 \text{ (bubble)} + 10 \text{ (bubble)} \right] \tag{3.8.2}$$

The associate diagram gives the following contribution

$$(1, -1) 2\lambda^2 \text{ (bubble)} \tag{3.8.3}$$

Diagram has the same topological structure as diagram and gives the following contribution

$$(1, -1) 2 \text{ (bubble)} \tag{3.8.4}$$

§3.9 Diagrams with only contribution

We shall list all the other independent diagrams that give only logarithmic divergent integral and a three-line-bubble.

$$\begin{array}{ll}
 \text{Diagram 1} \quad (1,-1)(-1) \text{ } \text{\textcircled{X}} & \text{Diagram 2} \quad (1,-1)(-1) \text{ } \text{\textcircled{X}} \\
 \text{Diagram 3} \quad (1,-1)(-1) \text{ } \text{\textcircled{X}} & \text{Diagram 4} \quad (1,-1) \text{ } \text{\textcircled{X}} \\
 \text{Diagram 5} \quad (1,-1) 2 \text{ } \text{\textcircled{X}} & \text{Diagram 6} \quad (1,-1)(-2) \text{ } \text{\textcircled{X}} \\
 \text{Diagram 7} \quad (1,-1)(-1) \text{ } \text{\textcircled{X}} & \text{Diagram 8} \quad (1,-1) \text{ } \text{\textcircled{X}} \quad (3.9.1)
 \end{array}$$

Now we want to demonstrate that this type of divergent integral, ie., $\text{\textcircled{X}}$, vanishes upon summation. This task can be accomplished by using only Jacobi-identity. In other words we want to show that


$$\begin{array}{l}
 2 \text{ } \text{Diagram 1} - 2 \text{ } \text{Diagram 2} - 4 \text{ } \text{Diagram 3} + 4 \text{ } \text{Diagram 4} - 4 \text{ } \text{Diagram 5} \\
 + 4 \text{ } \text{Diagram 6} - 4 \text{ } \text{Diagram 7} + 4 \text{ } \text{Diagram 8} + 10 \text{ } \text{Diagram 9} - 10 \text{ } \text{Diagram 10} \\
 + 2 \text{ } \text{Diagram 11} - 4 \text{ } \text{Diagram 12} - 12 \text{ } \text{Diagram 13} + 12 \text{ } \text{Diagram 14} = 0 \quad (3.9.2)
 \end{array}$$


It is easy to see that




$$\begin{array}{l}
 \text{Diagram 9} + \text{Diagram 12} = \text{Diagram 1} \\
 \text{Diagram 10} - \text{Diagram 11} = -\text{Diagram 1} \\
 \text{Diagram 11} - \text{Diagram 12} = -\text{Diagram 1} \\
 \text{Diagram 5} = \text{Diagram 7} \quad , \quad \text{Diagram 13} = \text{Diagram 1} \quad (3.9.3)
 \end{array}$$



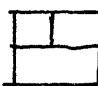

The above iso-spin identities are a simple result of Jacobi-identity and normalization of the three-vector-meson-line vertex. Applying these identities in sequence, we get


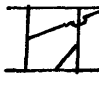


$$-8 \text{ } \text{Diagram 1} + 8 \text{ } \text{Diagram 1} = 0 \quad (3.9.4)$$




§3.10 Diagrams with only  contribution.

We shall list all the other independent diagrams that give only double logarithmic divergent integrals and a bubble, i.e., . For the sake of convenience we omit the integrals.

They are:  $(1,0)(-\frac{1}{2})$,  $(1,0)(-\frac{1}{2})$,  $(1,0)(-1)$

 $(1,0)(-\frac{1}{2})$,  $(1,0)(-\frac{1}{4})$,  $(1,0)(-\frac{1}{2})$,  $(1,-1)(-\frac{1}{2})$,

 $(1,-1)(\frac{1}{4})$,  $(1,-1)(\frac{1}{2})$,  $(1,-1)(\frac{1}{2})$,  $(1,-1)(-1)$,

 $(1,-1)(-1)$,  $(1,-1)$,  $(0,-1)(\frac{1}{2})$ (3.10.1)

We would like to point out that by virtue of the Jacobi-identity, this type of divergent integral also vanishes. The sum of all double logarithmic divergent integral is

$$\begin{aligned} & \left\{ (1,0) \left[2 \left(\text{diag}_1 - \text{diag}_2 - 2 \text{diag}_3 - \text{diag}_4 - \text{diag}_5 - \text{diag}_6 + \text{diag}_7 \right) \right. \right. \\ & \quad \left. \left. - 2 \text{diag}_8 + 2 \text{diag}_9 - 6 \text{diag}_{10} + 8 \text{diag}_{11} + 6 \text{diag}_{12} \right] \right. \\ & \quad \left. + (1,-1) \left[2 \text{diag}_{13} - 9 \text{diag}_{14} \right] + \text{s-u symmetry terms} \right\} \\ & + (1,-1) \left[6 \text{diag}_{15} - 8 \text{diag}_{16} - \text{diag}_{17} - \text{diag}_{18} + 2 \text{diag}_{19} + 2 \text{diag}_{20} \right. \\ & \quad \left. - 2 \text{diag}_{21} + \text{diag}_{22} \right] \end{aligned} \quad (3.10.2)$$


We shall use the following identities:

$$\begin{aligned} & \left(\text{diag}_{23} + \text{diag}_{24} \right) = \text{diag}_{25}, \quad \left(-\text{diag}_{26} + \text{diag}_{27} \right) = \text{diag}_{28}, \\ & \text{diag}_{29} = \text{diag}_{30} + \text{diag}_{31}, \quad \left(-\text{diag}_{32} + \text{diag}_{33} \right) = \text{diag}_{34}, \\ & \left(-\text{diag}_{35} + \text{diag}_{36} \right) = \text{diag}_{37}, \quad \left(\text{diag}_{38} - \text{diag}_{39} \right) = -\text{diag}_{40}, \\ & \text{diag}_{41} + \text{diag}_{42} = \text{diag}_{43}. \end{aligned} \quad (3.10.3)$$

Substitute (3.10.3) into (3.10.2) we have

$$\left\{ (1,0) \left[-7 \text{diag}_{44} - 5 \text{diag}_{45} - \text{diag}_{46} + 2 \text{diag}_{47} - 6 \text{diag}_{48} + 8 \text{diag}_{49} \right] \right.$$


$$\begin{aligned}
 & + (1, -1) \left\{ 2 \left[\text{diagram 1} \right] - 7 \left[\text{diagram 2} \right] \right\} + \text{s-u symmetry terms} \\
 & + (1, -1) \left\{ 6 \left[\text{diagram 3} \right] - 6 \left[\text{diagram 4} \right] + \left[\text{diagram 5} \right] + \left[\text{diagram 6} \right] - 2 \left[\text{diagram 7} \right] + \left[\text{diagram 8} \right] \right\} \\
 & = \left\{ (1, 0) \left[-7 \left[\text{diagram 9} \right] - 5 \left[\text{diagram 10} \right] + 2 \left[\text{diagram 11} \right] \right] + \text{s-u symmetry terms} \right\} \\
 & + (1, -1) \left\{ 4 \left[\text{diagram 12} \right] + 7 \left[\text{diagram 13} \right] - 12 \left[\text{diagram 14} \right] + \left[\text{diagram 15} \right] \right\} \\
 & = (1, -1) \left[-5 \left[\text{diagram 16} \right] - 5 \left[\text{diagram 17} \right] - 5 \left[\text{diagram 18} \right] + 5 \left[\text{diagram 19} \right] \right] = 0
 \end{aligned}$$

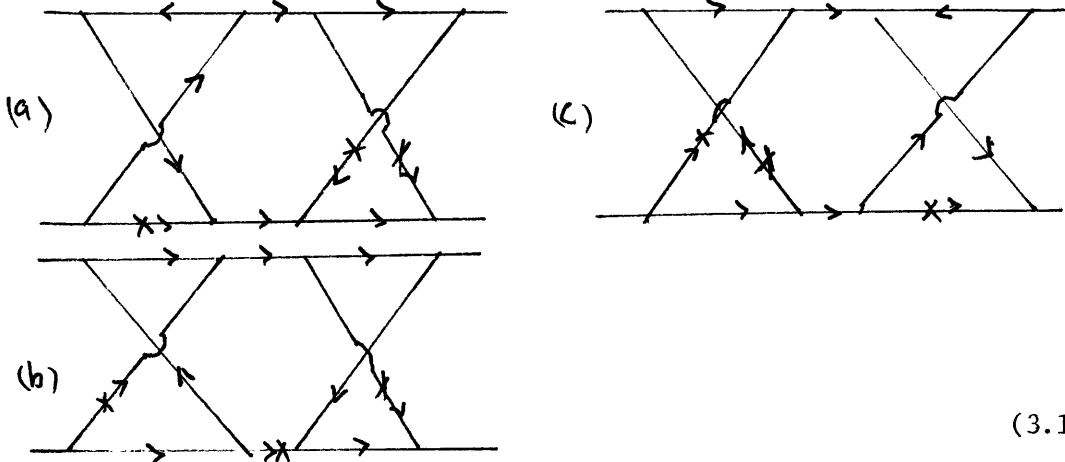
That is to say, the sum of all  terms vanishes.

§3.11 The multi-vector meson exchange diagrams.


In the eighth order, there are 24 multi-vector meson exchange diagrams but only four of them give contributions. They are



There are three flow diagrams for diagram 




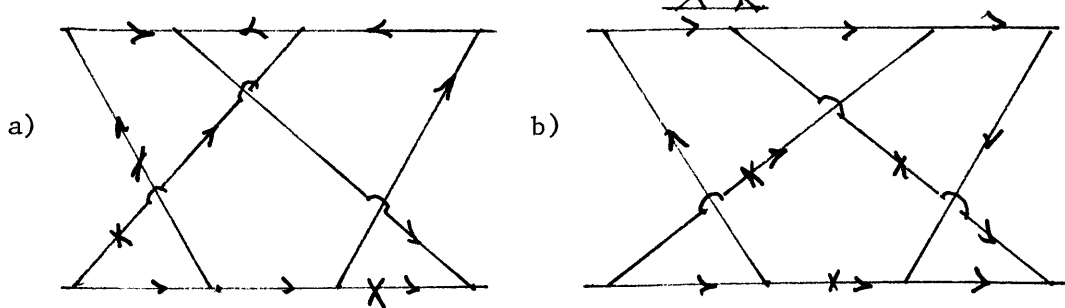
(3.11.1)

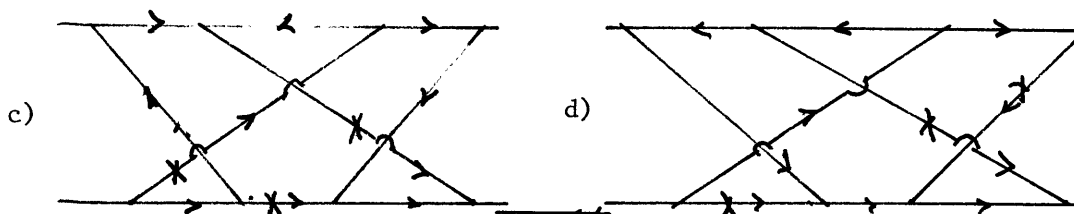
The contribution from diagram  is

$$\left[\text{diagram symbol} \right] (1, -1) (-4) \text{ } \text{diagram symbol}$$

(3.11.2)

There are four flow diagrams for diagram 





The contribution from diagram is

$$\text{Diagram c)} (1, -1) (4) \text{ } \text{ } \quad (3.11.3)$$

Using Jacobi-identity we have

$$\text{Diagram 1} - \text{Diagram 2} + \text{Diagram 3} - \text{Diagram 4} = \text{Diagram 5} \quad (3.11.4)$$

The total contribution from all the multi-vector-meson exchange, therefore, is

$$\text{Diagram 5} (1, -1) (-4) \text{ } \text{ } \quad (3.11.5)$$

For the tenth order multi-vector meson exchange diagrams, the iso-spin factor of the sum of their contribution is

For the next higher order, we just add one more bar parallel to the last bar added and so on. Now it is easy to see multi-vector meson exchange diagrams of order larger than four do not contribute to I=1 channel.

§3.12 The cancellation of terms

Let us add first all the contributions from diagrams of the first kind.

The sum of the coefficients is

$$\left\{ (1, 0) \left[\text{Diagram 1} (7\frac{1}{4}\Delta^2 + 11\lambda^2) + \text{Diagram 2} (1-\frac{1}{2})(6\frac{1}{2}\Delta^2 + 11\lambda^2) + \text{Diagram 3} (-2(2\Delta^2 + 3\lambda^2)) \right] + \text{s-u symmetric terms} \right\} + (1, -1) \left[\text{Diagram 4} 2(2\Delta^2 + 3\lambda^2) + \text{Diagram 5} (\frac{1}{2})(6\frac{1}{2}\Delta^2 + 11\lambda^2) \right] \quad (3.12.1)$$

The Jacobi-identity reduces (3.12.1) to

$$(1, 0) \text{Diagram 1} (-\frac{1}{2})\lambda^2 + (0, -1) \text{Diagram 2} (-\frac{1}{2})\lambda^2 \quad (3.12.2)$$

Now we sum up the rest of the terms. The sum of the coefficients is

$$(1, 0) \lambda^2 \left[3 \text{Diagram 1} - 2 \text{Diagram 2} - 2 \text{Diagram 3} + \frac{1}{2} \text{Diagram 4} \right] + \text{s-u symmetry terms.} \quad (3.12.3)$$


The Jacobi-identity reduces (3.12.3) to

$$(1, 0) \frac{\Lambda^2}{2} [\text{Diagram 1} + 2 \text{Diagram 2}] + \text{s-u symmetry terms.} \quad (3.12.4)$$

Adding (3.12.2) and (3.12.4) together we get

$$(1, -1) \frac{\Lambda^3}{2} [\text{Diagram 3} + \text{Diagram 4} + \text{Diagram 5}], \quad (3.12.5)$$


which is zero.

§3.13 The cancellation of  terms

Let us first add all the contributions from diagrams which have only vector-meson propagators and F-P ghost propagators. The sum of coefficients of such terms is

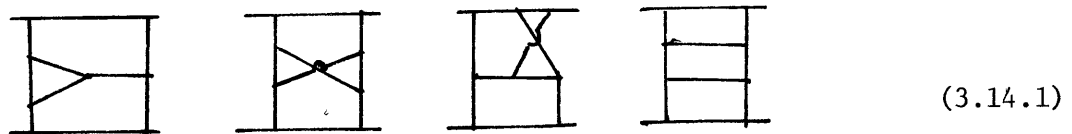
$$(1, 0) [\text{Diagram 6} (-3) + \text{Diagram 7} 8 - 5 \text{Diagram 8}] + \text{s-u symmetry term} \\ + (1, -1) \text{Diagram 9} (3) \quad (3.13.1)$$

We can easily see that (3.13.1) is zero by virtue of Jacobi-identity.

The sum of coefficients of  from the rest of the diagrams is also zero. We thus show that all divergent integrals vanish after summing up all the diagrams in the eighth order

§3.14 Terms of order greater than $S(\ln S)^3$.

We have mentioned in the beginning of this chapter that the terms of order greater than $S(\ln S)^3$, such as S^2 , $S^2 \ln S$ and S^3 , do not appear in our calculation. Here we point out that if one calculates Feynman diagrams individually, instead of grouping each Feynman diagram with its associate diagrams, such terms do occur. The reader can easily see such terms in the following diagrams:



§3.15 Conclusion and Discussion

In the last section, we have shown that all the divergent integrals cancel. The convergent integrals, after adding up, take the following

form:

$$\begin{aligned}
 \mathcal{M}_{\nu\nu}^{(8)} = & -g^8(1,1) \left\{ \text{diagram} (\Delta^2 + \lambda^2)^2 \mathbb{I} \right. \\
 & -g^8(1,-1) \left\{ \text{diagram} \frac{1}{4} [(2\Delta^2 + 3\lambda^2)(\mathbb{H} + \mathbb{X}) \right. \\
 & \quad \left. - 2\lambda^2(2\Delta^2 + 3\lambda^2)(\mathbb{H} + \mathbb{X}) + \lambda^4(\mathbb{H} + \mathbb{X})] \right. \\
 & \quad \left. + \text{diagram} 2[-(4\Delta^2 + 7\lambda^2)\mathbb{M} + \lambda^2(\mathbb{H} + \mathbb{X})] \right. \\
 & \quad \left. + (\text{diagram} + \text{diagram}) + \text{diagram} \right\}
 \end{aligned}
 \tag{3.15.1}$$

The results of 2nd - 8th order calculations indicate that

$$F_1 = G_1 \tag{3.15.2}$$

and

$$F_0 = 3/8 G_0 \tag{3.15.3}$$

The amplitude G_1 is the simplest one. Up to the 8th order, the leading terms of G_1 form the first four terms in the perturbation series of a Regge pole term

$$G_1 \sim \frac{2g^2}{\Delta^2 + \lambda^2} s^{\alpha_1} (1 - e^{-\lambda\pi\alpha_1}) \tag{3.15.4}$$

where g is the coupling constant, λ is the mass of the vector meson, and

$$\alpha_1 = 1 - g^2(\Delta^2 + \lambda^2) \text{diagram} \tag{3.15.5}$$

Notice that the Regge pole α_1 which passes through the vector meson pole ($\alpha_1 = 1$ and the coefficient of s^{α_1} in (4) blows up at $t = -\lambda^2$) is of $I = 1$, and has an odd signature. This suggests that α_1 is the Reggerization of the vector meson.

The other invariant amplitudes are more complex:

$$\begin{aligned}
 G_0 \sim & 4\pi g^4 s \left[\frac{a}{\Delta^2 + \frac{5}{4}\lambda^2} + \left(\frac{-a^2}{\Delta^2 + \frac{5}{4}\lambda^2} + 4A \right) g^2 \ln s \right. \\
 & \left. + \left(\frac{a^3}{\Delta^2 + \frac{5}{4}\lambda^2} - 8aA + 4B \right) g^4 \frac{(\ln s)^2}{2!} \right]
 \end{aligned}
 \tag{3.15.6}$$

$$G_2 \sim 2\pi i g^4 S \left[\frac{b}{\Delta^2 + 2\lambda^2} + \left(\frac{b^2}{\Delta^2 + 2\lambda^2} - 4A \right) g^2 \ln S \right. \\ \left. + \left(\frac{b^3}{\Delta^2 + 2\lambda^2} - 8bA + 8B \right) g^4 \frac{(\ln S)^2}{2!} \right], \quad (3.15.7)$$

in the above

$$a = (2\delta^2 + \frac{5}{2}\lambda^2) \Phi$$

$$b = (\Delta^2 + 2\lambda^2) \Phi$$

$$A = \Phi$$

and

$$B = \Phi + \Phi \quad (3.15.8)$$

We now compare the high-energy behavior in Yang-Mills theory with that in Q. E. D. (1) Just like in Q.E.D., all integrals over the transverse momenta are convergent, and all $\ln S$ factors come from integrations over the phase space of the longitudinal momenta. This means that the energy dependence of cross sections is a consequence of the creation of pionization products; (2) first like in Q. E. D. the convergence of integrations over transverse momenta is a result of spectacular cancellations among sets of diagrams. Such cancellations appear to depend on only the group properties of gauge theories, and are not restricted to the SU(2) group treated here. (3) Unlike in Q. E. D. the largest term in each perturbation order is real. It is also true of $I = 1$ in the t - channel. In the eighth order, for example, F_1 is of the order of $S(\ln S)^3$, while F_0 is of the order of $S(\ln S)^2$; (4) This means that, in each perturbation order, $\text{Re } \mathcal{M} / \text{Im } \mathcal{M}$ approaches infinity as $S \rightarrow \infty$, and the cross-section for a charge exchange reaction is equal to the elastic cross-section. Such a behavior is contradictory to the well-found experimental facts.¹⁴⁾ It is therefore

gratifying to see that such large terms in F_1 appear to cancel one another as we sum over all perturbation orders. More precisely, the 2nd - 8th order results suggest that these terms add up to the Regge pole term in (3.15.4) with $\alpha_1 < 1$ in the physical region of the s - channel. This is to be compared with the situation in Q. E. D. where the real part of the elastic scattering amplitude due to the exchange of a photon does not reggeize.

Finally, we want to point out that our method of expressing both the iso-spin factors and the transverse momentum integrals in diagrammatic forms has the following advantages:

1) A complicated transverse momentum integral is represented by a linear sum of simple diagrams.

2) The iso-spin factor associated with a Feynman diagram is represented by this same Feynman diagram. This helps to remind us of the origins of a particular transverse momentum integral.

3) It enables us to demonstrate explicitly the role that the Jacobi-identity plays in the cancellation of divergent integrals. It also makes it trivial to extend the result to arbitrary non-abelian gauge field theories.

4) The decomposition of an integral into a sum of convergent integrals and divergent integrals (which will be cancelled out upon summing up all of the contributions of the same order) provides us with a much faster method to obtain the final results by simply ignoring all divergent integrals after the decomposition:

Chapter IV Higher order diagrams

§4.1 The necessity of calculating higher order diagrams

The eighth order calculation and its results have not given us sufficient information to predict what higher order terms will be. For the $I = 1$ channel although we conjecture that it is a kegge pole, we are not certain. For $I = 0, 2$ channels, the situation is even more so.

We note that the number of diagrams increases very rapidly, as a result of the three line Yang-Mills vertex. In the second order we have only one diagram to calculate; in the fourth order we have 2; in the sixth order we have about 20; and in the eighth order we have over 200. It would not be surprising that in the tenth order we have over 2,000 diagrams to calculate. Even if we could calculate them all, how about the twelfth order and higher order diagrams. We also notice that in (3.7.45) and (3.15.1) only those diagrams with convergent integral contributions enter these final results. It appears that we are doing a lot of unnecessary calculations.

§4.2 Convergent part of an integral and convergent diagram

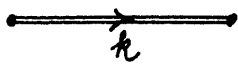
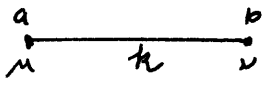
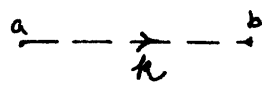
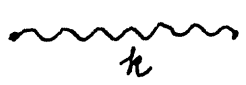
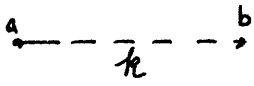
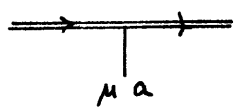
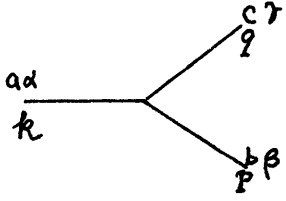
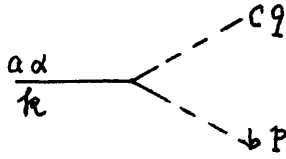
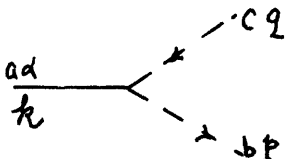
As we have mentioned before we should find a way to obtain the final result directly. If we believe that the final answer of each order is a sum of convergent transverse integrals, we can calculate just those diagrams which give convergent integral contributions and get the final results very quickly. Since we are concerned only with convergent integrals, regions which give divergent integrals can be ignored. We notice that the possibility of convergence of a transverse momentum integral can be determined by the structure of the diagram considered. We define a diagram is convergent if its structure gives convergent integral contributions. So the calculation of higher order diagrams is reduced basically to finding a fast way to eliminate divergent diagrams.

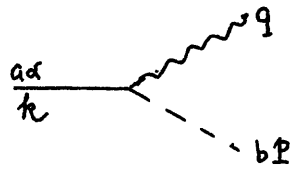
REFERENCES

- 1) H. Cheng and T. T. Wu, Phys. Rev. Lett. 24, 1456 (1970) and earlier papers quoted therein.
- 2) S. R. Amendolia et al., Phys. Lett. 44B, 119 (1973).
- 3) C. N. Yang and R. Mills, Phys. Rev. 96 191 (1954).
- 4) For a review, see, e.g. B. W. Lee, in Proceedings of the Sixteenth International Conference on High Energy Physics, The University of Chicago and National Accelerator Laboratory, 1972, edited by J. D. Jackson and A. Roberts (National Accelerator Laboratory, Batavia, Ill., (1973).
- 5) D. J. Gross and F. Wilczek, Phys. Rev. Lett. 30, 1346 (1973); G. t'Hooft, unpublished.
- 6) Marcel Froissart, Phys. Rev. Vol. 123, No. 3, 1053 (1961).
- 7) H. T. Nieh and York-Peng Yao, Phys. Rev. Lett. 32, No. 19, 1074 (1974).
- 8) B. M. McCoy and T. T. Wu, Phys. Rev. Lett. 35 604 (1975). Harvard University preprint ITP-SB-75-21.
- 9) t'Hooft and Veltman, proceedings of Colloquium on Renormalization of Yang-Mills Fields and Applications to particle Physics, Marseille, France, 1972, edited by C. P. Korthals-Atles (C.N.S., Marseille, France, 1972).
- 10) Popov and Faddeev, Perturbation theory for gauge invariant Fields, Kiev, ITP report.
- 11) Patrick S. Yeung, MIT, preprint CTP No. 520.
- 12) H. Cheng and T. T. Wu, Phys. Rev. 182, 1899 (1969).
- 13) H. Cheng, private communication.
- 14) The experiment we refer to is $P + \pi^- \rightarrow n + \pi^0$

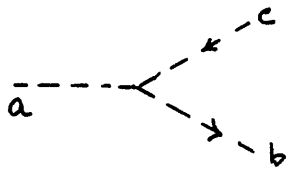
Appendix A Feynman Rules

The Feynman rules have been given explicitly by t'Hooft and Veltman⁹⁾. We list only the case of Feynman gauge where there are no $k_\mu k_\nu$ terms in the propagator for the Yang-Mills field.

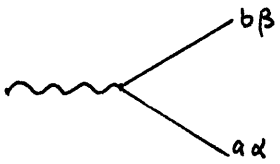
	$\frac{-(\not{k} + M)}{k^2 - M^2 + i\epsilon}$	Fermion propagator
	$\delta_{ab} \times \frac{g_{\mu\nu}}{k^2 - \lambda^2 + i\epsilon}$	Vector-meson propagator (Yang-Mills field)
	$\delta_{ab} \times \frac{-1}{k^2 - \lambda^2 + i\epsilon}$	F-P ghost propagator (-1 for every closed loop)
	$\frac{-1}{k^2 - \mu^2 + i\epsilon}$	$\mu^2 = 40\lambda^2$ Z - propagator
	$\delta_{ab} \times \frac{-1}{k^2 - \lambda^2 + i\epsilon}$	γ - propagator
	$\frac{1}{2} \tau_a \times g \gamma_\mu$	Fermion-Vector Boson Vertex
	$i\epsilon_{abc} \times g \left\{ g_{\alpha\beta} (q-k)_\gamma + g_{\alpha\gamma} (k-p)_\beta + g_{\beta\gamma} (p-q)_\alpha \right\}$	Yang-Mills Three-line Vertex
	$i\epsilon_{abc} \times g \frac{1}{2} (p-q)_\alpha$	
	$i\epsilon_{abc} \times g (-p)_\alpha$	



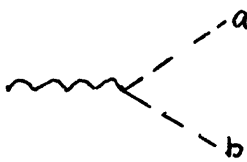
$$\delta_{ab} \times g \frac{-i}{2} (P - Q)_\alpha$$



$$i \epsilon_{abc} \times g \left(\frac{-i}{2}\right) \lambda$$



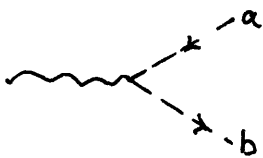
$$\delta_{ab} \times g g_{\alpha\beta} \lambda$$



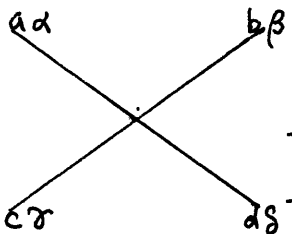
$$\delta_{ab} \times g (-2\alpha\lambda)$$



$$g (-6\alpha\lambda)$$

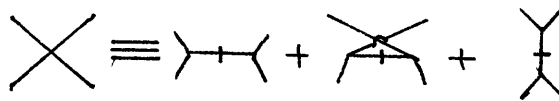
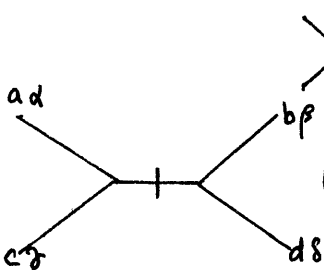


$$\delta_{ab} \times g \left(\frac{-\lambda}{2}\right)$$



$$\begin{aligned} & (i\epsilon_{gba})(i\epsilon_{gca}) \times (-g^2) (g_{\alpha\gamma} g_{\beta\delta} - g_{\alpha\delta} g_{\beta\gamma}) \\ & + (i\epsilon_{gac})(i\epsilon_{gdb}) \times (-g^2) (g_{\alpha\beta} g_{\gamma\delta} - g_{\alpha\delta} g_{\beta\gamma}) \\ & + (i\epsilon_{gad})(i\epsilon_{gcb}) \times (-g^2) (g_{\alpha\beta} g_{\gamma\delta} - g_{\alpha\gamma} g_{\beta\delta}) \end{aligned}$$

Yang-Mills Four-line Vertex



$$(i\epsilon_{gac})(i\epsilon_{gdb}) \times (-g^2) (g_{\alpha\beta} g_{\gamma\delta} - g_{\alpha\delta} g_{\beta\gamma})$$

$\delta_{ab} \delta_{cd} \times g^2(\frac{1}{2}) g_{\alpha\beta}$

$\delta_{ab} \times g^2 \frac{1}{2} g_{\alpha\beta}$

$(\delta_{ab} \delta_{cd} + \delta_{ac} \delta_{bd} + \delta_{ad} \delta_{bc}) \times g^2(-\sigma)$

$\delta_{ac} \delta_{bd} \times g^2(-\sigma)$

$\delta_{ab} \times g^2(-\sigma)$

$g^2(-3\sigma)$

$g^2(-\sigma)$

We note that any propagator or any three-line vertex is a product of an isospin factor (before the sign \times) and a time space factor. But some four-line vertices have somewhat different structure. However, we could think of such four-line vertex as a sum of four-line vertices which can be factorized into a product of an isospin factor and a time-space factor.

A factorizable four-line vertex is denoted by two connecting three-line-vertices with a bar on the connecting line. The notations are assigned in such a way that the unbarred connecting two three-line vertices and the barred connecting two three-line-vertices have exactly the same iso-spin factor.

Appendix B The Eighth order contributing diagrams

We list the independent structures (see §2.4 and §2.5) of all the contributing diagrams below:

